



HAL
open science

Fully discrete loosely coupled Robin-Robin scheme for incompressible fluid-structure interaction: stability and error analysis

Erik Burman, Rebecca Durst, Miguel Angel Fernández, Johnny Guzmán

► **To cite this version:**

Erik Burman, Rebecca Durst, Miguel Angel Fernández, Johnny Guzmán. Fully discrete loosely coupled Robin-Robin scheme for incompressible fluid-structure interaction: stability and error analysis. *Numerische Mathematik*, 2022, 151, pp.807-840. 10.1007/s00211-022-01295-y . hal-02893444

HAL Id: hal-02893444

<https://hal.science/hal-02893444>

Submitted on 8 Jul 2020

HAL is a multi-disciplinary open access archive for the deposit and dissemination of scientific research documents, whether they are published or not. The documents may come from teaching and research institutions in France or abroad, or from public or private research centers.

L'archive ouverte pluridisciplinaire **HAL**, est destinée au dépôt et à la diffusion de documents scientifiques de niveau recherche, publiés ou non, émanant des établissements d'enseignement et de recherche français ou étrangers, des laboratoires publics ou privés.

FULLY DISCRETE LOOSELY COUPLED ROBIN-ROBIN SCHEME FOR INCOMPRESSIBLE FLUID-STRUCTURE INTERACTION: STABILITY AND ERROR ANALYSIS

ERIK BURMAN, REBECCA DURST, MIGUEL A. FERNÁNDEZ, AND JOHNNY GUZMÁN

ABSTRACT. We consider a fully discrete loosely coupled scheme for incompressible fluid-structure interaction based on the time semi-discrete splitting method introduced in [Burman, Durst & Guzmán, *arXiv:1911.06760*]. The splitting method uses a Robin-Robin type coupling that allows for a segregated solution of the solid and the fluid systems, without inner iterations. For the discretisation in space we consider piecewise affine continuous finite elements for all the fields and ensure the inf-sup condition by using a Brezzi-Pitkäranta type pressure stabilization. The interfacial fluid-stresses are evaluated in a variationally consistent fashion, that is shown to admit an equivalent Lagrange multiplier formulation. We prove that the method is unconditionally stable and robust with respect to the amount of added-mass in the system. Furthermore, we provide an error estimate that shows the error in the natural energy norm for the system is $\mathcal{O}(\sqrt{T}(\sqrt{\Delta t} + h))$ where T is the final time, Δt the time-step length and h the space discretization parameter.

1. INTRODUCTION

The computational solution of fluid-structure interaction problems remains a challenging problem. Indeed the combination of the continuity requirement of velocities and stresses across the interface with the incompressibility constraint leads to a very stiff problem. In order to be able to use optimised solvers and existing codes for the fluid and the solid sub-systems and to simplify the handling of geometric nonlinearities it is appealing to use a loosely coupled (or explicit coupling) where the solid and fluid systems are solved sequentially, passing information across the coupling interface at discrete time levels, without iterating between the sub-systems within one time-step. This partitioned solution procedure has been very successful in the context of aeroelasticity (see [15]), but in other applications, depending on the geometry of the computational domain or the physical parameters, it has been shown to suffer from severe stability problems (see [14]). In particular, in applications where the fluid-solid density ratio is close to one any naive decoupling of the fluid-solid system to form a loosely coupled scheme is known to be unstable.

In this paper, we revisit the loosely coupled scheme based on a Robin-Robin type coupling for the coupling of an incompressible fluid with a thick-walled solid, introduced in [13, Algorithm 4]. Recently (see [11]), this method was analysed in the time semi-discrete framework, i.e. independent of any space mesh parameter, and was shown to be stable independent of the fluid-solid density ratio. In particular, the dependence of the Robin-coefficient on the inverse of the space mesh parameter (and the pressure stabilizer necessary for the stability arguments of [13]) were eliminated. The splitting error of the scheme could then be shown to be $\mathcal{O}(\sqrt{T}\sqrt{\Delta t})$. Note the absence of exponential growth of perturbations in time (with respect to T). The success in [11] relies on the fact that, at the continuous level, one can use the Robin condition in strong form, provided the solution of the time-discretised fluid system is sufficiently regular. Indeed, if $\alpha \in \mathbb{R}^+$ denotes the Robin parameter, \mathbf{u} , \mathbf{q} , $\sigma_f(\mathbf{u}, p)$ and $\sigma_s(\boldsymbol{\eta})$ are the fluid and solid velocities and stresses at some time-levels, * superscripts indicate a shift by one time-step, and Σ stands for the fluid-solid interface, the Robin type coupling condition in the fluid formally reads

$$\sigma_f(\mathbf{u}, p)n_f + \alpha \mathbf{u} = \alpha \mathbf{q} + \sigma_f(\mathbf{u}^*, p^*)n_f \quad \text{on } \Sigma.$$

A key ingredient in the stability analysis of the time semi-discretized method is to write

$$(1.1) \quad \alpha(\mathbf{u} - \mathbf{q}) = \sigma_f(\mathbf{u}^*, p^*)n_f - \sigma_f(\mathbf{u}, p)n_f.$$

Assuming sufficient regularity, the discrepancy in the velocities across the interface can then be replaced by the increment of the stresses, which is used to obtain stability. It should however be noted that, at the discrete level, the relation (1.1) does not hold true in general, if standard finite elements are used for space discretization. Indeed, the stresses will be discontinuous across element boundaries and on polygonal approximations of the boundary also n_f will jump. It follows that the equality (1.1) can not be used and that a fully discrete scheme based on the time-discrete approach of [11] has to be carefully designed, with a discretization of the stresses that is compatible with the loosely coupled scheme.

Drawing on ideas from [28] (see also [13, Algorithm 3]) we consider a variational consistent representation of the interfacial fluid-stresses (i.e., as the classical fluid variational residual involving a fluid-sided lifting operator) and show that the resulting scheme can be recast as a Lagrange multiplier method. Matching the trace spaces of the solid and fluid velocities, with that of the multiplier, allows us to recover a relation similar to (1.1) in the fully discrete framework. A complete a priori error analysis for the fully discrete method, using piecewise affine approximation for all the unknowns is then carried out resulting in an error estimate of $\mathcal{O}(\sqrt{T}(\sqrt{\Delta t} + h))$ in the natural norm. This shows that our extension to the fully discrete case of the method proposed in [11] is optimal, with no added conditions on the discretization parameters or exponential growth of perturbations. To the best of our knowledge this is the first fully discrete loosely coupled method for fluid-structure interaction problems with thick-walled solids that allows for error estimates reflecting the splitting error and the approximation order of the finite element space, without any conditions on the physical or discretization parameters.

1.1. Overview of previous work. The source of instability occurring in loosely coupled methods was identified by Causin *et al.* [14] as the so-called added-mass effect, see also [28, 23]. They also showed that the alternative, solving the interface coupling implicitly (strong coupling) and in a partitioned iterative fashion, on the other hand is very costly in this regime, due to the stiffness of the coupling. A first step in the direction of decoupling the two systems were the semi-implicit coupling schemes (see [19, 31, 3, 1, 8]), where the implicit part of the coupling, typically the elasticity system and the fluid incompressibility (i.e., the added-mass), guarantees stability, and the explicit step (transport in the fluid and geometrical non-linearities) reduces the computational cost. Such splitting methods nevertheless retain an implicit part, although of reduced size, and require a specific time-stepping in the fluid. Provably stable fully explicit coupling was first achieved by Burman and Fernández [12] using a formulation based on Nitsche's method, drawing on an earlier, fully implicit formulation by Hansbo *et al.* [26]. Stability was achieved by the addition of a temporal pressure stabilization that relaxed incompressibility in the vicinity of the interface. Although the proposed scheme was proved to be stable irrespectively of the added-mass effect, it suffered from a strong splitting error of order $O(\Delta t/h)$ leading to a convergent scheme only for $\Delta t = \mathcal{O}(h^\alpha)$ with $\alpha > 1$. The source of this consistency error was the penalty term of the Nitsche formulation. In a further development Burman and Fernández compared the Nitsche based method with a closely related scheme using a Robin type splitting procedure [13]. Robin type domain decomposition had already been applied for the partitioned solution of strong coupling by Badia *et al.* [2, 29, 24] and Robin related explicit coupling was proposed in [4], but without theoretical justification. The loosely coupled scheme based on Robin type coupling of [13] was proved to be stable, but with similar shortcomings as the Nitsche based method. Since then several works [22, 10, 7, 21] have studied the loosely coupled schemes for the interaction of an incompressible fluid and a thick-walled solid. At best (see [22, 21]) their error analysis results in estimates of order $O(\Delta t/\sqrt{h})$ under various (mild) conditions on the discretization parameter. Observe that these latter references extend techniques designed for the case of an incompressible fluid interacting with a thin-walled solid (see [18, 16]) to the case of the coupling with a thick-walled solid. When preparing to submit the present work we came across a report recently posted to arxiv by Seboldt and Bukač [33],

where a method using Robin-conditions in a loosely coupled scheme similar to the one introduced in [11] was analyzed. The main differences in our work compared to theirs is that we use residual lifting, or Lagrange multipliers, for the interface stresses and prove error estimates without conditions on the discretization parameters and without exponential growth of the stability constant in time. In their work on the other hand they derive a stability estimate for the time semi-discretized problem where a moving domain is accounted for and use arbitrary inf-sup stable finite element spaces in the error analysis.

1.2. Coupling of an incompressible fluid with a thin-walled solid. Let us finally mention the case of an incompressible fluid coupled with a thin-walled solid, i.e. a solid that is modeled on a domain of co-dimension 1 compared to the fluid system. This system is simpler and many coupling schemes have been developed and analysed starting with the seminal work of Guidoboni *et al.* [25], for instance [18, 16, 20, 9, 34, 30].

Since the solid model is restricted to the $(d - 1)$ dimensional interface domain the solid velocities interact with the fluid everywhere in their domain of definition. This means that there is no relaxation times associated with propagation of waves in the direction perpendicular to the interface. Therefore the stability of the solid system holds on the $d - 1$ -dimensional interface and not in the d -dimensional bulk. The fundamental idea for stability is to implicitly integrate the solid inertial contributions within the fluid, through a Robin-type interface condition (which avoids the above mentioned added-mass issues) and appropriately extrapolate the remaining solid contributions for accuracy (see, e.g., [18, 16]). Nevertheless, when considering thick-walled solids, typically a trace inequality must be applied to control interface quantities using the stability in the bulk domain (see, e.g., [21]). This leads to the need of control of higher derivatives, or a loss of a negative power of the space mesh parameter. Therefore, when methods used for the coupling with thin-walled solids are extended to the thick-walled solid case, sub-optimal accuracy issues depending on the ratio of the time and space grid parameters result as in the examples in the previous section. In other words, time splitting with thick-walled solids suffers from more severe accuracy issues than in the thin-walled solid case.

2. THE LINEAR FLUID-SOLID INTERACTION PROBLEM

Let Ω_s and Ω_f be two polygonal domains with a matching interface $\Sigma = \partial\Omega_s \cap \Omega_f$. For simplicity, we assume that the interface Σ is a straight line. We also let $\Sigma_f = \Omega_f \setminus \Sigma$ and $\Sigma_s = \Omega_s \setminus \Sigma$. We consider the following coupled problem

$$(2.1) \quad \begin{cases} \rho_f \partial_t \mathbf{u} - \operatorname{div} \sigma_f(\mathbf{u}, p) = 0 & \text{in } (0, T) \times \Omega_f, \\ \operatorname{div} \mathbf{u} = 0 & \text{in } (0, T) \times \Omega_f, \\ \mathbf{u} = 0 & \text{on } (0, T) \times \Sigma_f, \end{cases}$$

$$(2.2) \quad \begin{cases} \rho_s \partial_t \mathbf{q} - \operatorname{div} \sigma_s(\boldsymbol{\eta}) = 0 & \text{in } (0, T) \times \Omega_s, \\ \mathbf{q} - \partial_t \boldsymbol{\eta} = 0 & \text{in } (0, T) \times \Omega_s, \\ \boldsymbol{\eta} = 0 & \text{on } (0, T) \times \Sigma_s, \end{cases}$$

$$(2.3) \quad \begin{cases} \mathbf{u} = \mathbf{q} & \text{on } (0, T) \times \Sigma, \\ \sigma_f(\mathbf{u}, p) \mathbf{n}_f + \sigma_s(\boldsymbol{\eta}) \mathbf{n}_s = 0 & \text{on } (0, T) \times \Sigma, \end{cases}$$

complemented with the following initial conditions:

$$\begin{aligned} \boldsymbol{\eta}(0, \cdot) &= \boldsymbol{\eta}_0 & \text{in } \Omega_s, \\ \mathbf{q}(0, \cdot) &= \mathbf{q}_0 & \text{in } \Omega_s, \\ \mathbf{u}(0, \cdot) &= \mathbf{u}_0 & \text{in } \Omega_f. \end{aligned}$$

Here, \mathbf{n}_i is the outward pointing normal to $\partial\Omega_i$ for $i = s, f$. The stress tensors are given by

$$\begin{aligned}\sigma_f(\mathbf{u}, p) &:= 2\mu\epsilon(\boldsymbol{\eta}) - p\mathbf{I}, \\ \sigma_s(\boldsymbol{\eta}) &:= 2L_1\epsilon(\boldsymbol{\eta}) + L_2(\operatorname{div} \boldsymbol{\eta})\mathbf{I}.\end{aligned}$$

Here μ is the viscosity of the fluid and L_1, L_2 are the Lamé constants of the solid, with $L_1 > 0$ and $L_2 \geq 0$. The solid and fluid densities are denoted ρ_s, ρ_f , respectively.

Let us define the following spaces

$$\begin{aligned}\mathbf{V}^s &:= \{\mathbf{v} \in \mathbf{H}^1(\Omega_s) : \mathbf{v} = 0 \text{ on } \Sigma_s\}, \\ \mathbf{V}^f &:= \{\mathbf{v} \in \mathbf{H}^1(\Omega_f) : \mathbf{v} = 0 \text{ on } \Sigma_f\}, \\ \mathbf{V}^g &:= L^2(\Sigma), \\ M^f &:= L_0^2(\Omega_f).\end{aligned}$$

We let

$$\boldsymbol{\lambda} := \sigma_f(\mathbf{u}, p)\mathbf{n}_f.$$

Then if we assume that $\boldsymbol{\lambda} \in L^2(\Sigma)$ we have that the solution of (2.1)-(2.3) satisfies the weak formulation: For $t > 0$, find $\mathbf{q}(t), \boldsymbol{\eta}(t) \in \mathbf{V}^s$, $\mathbf{u}(t) \in \mathbf{V}^f$, $\boldsymbol{\lambda}(t) \in \mathbf{V}^g$, $p(t) \in M^f$ satisfying

$$(2.4a) \quad \rho_s(\partial_t \mathbf{q}, \boldsymbol{\xi})_s + a_s(\boldsymbol{\eta}, \boldsymbol{\xi}) + \langle \boldsymbol{\lambda}, \boldsymbol{\xi} \rangle = 0 \quad \forall \boldsymbol{\xi} \in \mathbf{V}^s$$

$$(2.4b) \quad (\mathbf{q}, \boldsymbol{\phi})_s - (\partial_t \boldsymbol{\eta}, \boldsymbol{\phi})_s = 0 \quad \forall \boldsymbol{\phi} \in \mathbf{V}^s$$

$$(2.4c) \quad \rho_f(\partial_t \mathbf{u}, \mathbf{v})_f + a_f((\mathbf{u}, p), (\mathbf{v}, \theta)) - \langle \boldsymbol{\lambda}, \mathbf{v} \rangle = 0 \quad \forall (\mathbf{v}, \theta) \in \mathbf{V}^f \times M^f$$

$$(2.4d) \quad \langle \mathbf{u} - \mathbf{q}, \boldsymbol{\mu} \rangle = 0 \quad \forall \boldsymbol{\mu} \in \mathbf{V}^g.$$

Here $(\cdot, \cdot)_i$ is the L^2 inner-product on Ω_i , $i = s, f$. Also, $\langle \cdot, \cdot \rangle$ is the L^2 inner-product on Σ . Finally, the bilinear form a_f and a_s are respectively given by

$$\begin{aligned}a_f((\mathbf{u}, p), (\mathbf{v}, \theta)) &:= 2\mu(\epsilon(\mathbf{u}), \epsilon(\mathbf{v}))_f - (p, \operatorname{div} \mathbf{v})_f + (\operatorname{div} \mathbf{u}, \theta), \\ a_s(\boldsymbol{\eta}, \boldsymbol{\xi}) &:= 2L_1(\epsilon(\boldsymbol{\eta}), \epsilon(\boldsymbol{\xi}))_s + L_2(\operatorname{div} \boldsymbol{\eta}, \operatorname{div} \boldsymbol{\xi})_s\end{aligned}$$

and the induced elastic energy norm

$$\|\boldsymbol{\eta}\|_S^2 := a_s(\boldsymbol{\eta}, \boldsymbol{\eta}).$$

3. NUMERICAL METHOD

3.1. Time discretization: Robin-based loosely coupled scheme. We discretize the time interval $(0, T)$ with N sub-intervals (t_n, t_{n+1}) where $t_n = \Delta t n$, $T = t_N$ and Δt is the time-step length. We introduce the standard notation

$$\partial_{\Delta t} f^{n+1} := \frac{1}{\Delta t}(f^{n+1} - f^n), \quad f^{n+1/2} := \frac{1}{2}(f^{n+1} + f^n).$$

As mentioned in the introduction, a splitting method was introduced in [11] using a Robin-based procedure that solves two PDEs, sequentially, in each time step. Here we further discretize that method by applying a backward Euler method in the fluid and a mid-point scheme in the solid. This yields the time semi-discrete solution procedure reported in Algorithm 1, where $\alpha > 0$ denotes the so-called Robin parameter (user defined). Note that Algorithm 1 is nothing but the generalization of the genuine Robin-Robin explicit coupling scheme introduced in [13, Algorithm 4] to the case of a general Robin coefficient $\alpha > 0$ (i.e., the traditional Nitsche penalty parameter $\gamma\mu/h$ is replaced by α).

Unconditional energy stability and sub-optimal $\mathcal{O}(\sqrt{\Delta t})$ accuracy are derived in [11] for the PDE version of Algorithm 1, irrespectively of the value of $\alpha > 0$. The relation (3.2)₄ plays a fundamental role in the analysis of the method. The next section provides a fully discrete version of Algorithm 1 using a conforming finite element approximation in space.

Algorithm 1 Time semi-discrete, Robin-based, loosely coupled scheme (from [11]).

(1) Solid subproblem:

$$(3.1) \quad \begin{cases} \rho_s \partial_{\Delta t} \mathbf{q}^{n+1} - \operatorname{div} \sigma_s(\boldsymbol{\eta}^{n+\frac{1}{2}}) = 0 & \text{in } \Omega_s, \\ \partial_{\Delta t} \boldsymbol{\eta}^n = \mathbf{q}^{n+\frac{1}{2}} & \text{in } \Omega_s, \\ \boldsymbol{\eta}^{n+1} = 0 & \text{on } \Sigma_s, \\ \sigma_s(\boldsymbol{\eta}^{n+\frac{1}{2}}) n_s + \alpha \mathbf{q}^{n+\frac{1}{2}} = \alpha \mathbf{u}^n - \sigma_f(\mathbf{u}^n, p^n) n_f & \text{on } \Sigma. \end{cases}$$

(2) Fluid subproblem:

$$(3.2) \quad \begin{cases} \rho_f \partial_{\Delta t} \mathbf{u}^{n+1} - \operatorname{div} \sigma_f(\mathbf{u}^{n+1}, p^{n+1}) = 0 & \text{in } \Omega_f, \\ \operatorname{div} \mathbf{u}^{n+1} = 0 & \text{in } \Omega_f, \\ \mathbf{u}^{n+1} = 0 & \text{on } \Sigma_f, \\ \sigma_f(\mathbf{u}^{n+1}, p^{n+1}) n_f + \alpha \mathbf{u}^{n+1} = \alpha \mathbf{q}^{n+\frac{1}{2}} + \sigma_f(\mathbf{u}^n, p^n) n_f & \text{on } \Sigma. \end{cases}$$

3.2. Finite element approximation with fitted meshes. We assume that \mathcal{T}_h^i is a simplicial triangulation of Ω_i where $i = s, f$. We assume the meshes are quasi-uniform and shape-regular [5]. Furthermore, we assume that the meshes match on the interface Σ . We define the following finite element spaces:

$$\begin{aligned} \mathbf{V}_h^s &:= \{ \mathbf{v} \in \mathbf{V}^s : \mathbf{v}|_K \in \mathcal{P}^1(K), \forall K \in \mathcal{T}_h^s \}, \\ \mathbf{V}_h^f &:= \{ \mathbf{v} \in \mathbf{V}^f : \mathbf{v}|_K \in \mathcal{P}^1(K), \forall K \in \mathcal{T}_h^f \}, \\ \mathbf{V}_h^g &:= \{ \text{trace space of } \mathbf{V}_h^f \text{ on } \Sigma \}, \\ M_h^f &:= \{ v \in M^f : v|_K \in \mathcal{P}^1(K), \forall K \in \mathcal{T}_h^f \}. \end{aligned}$$

Here $\mathcal{P}^1(K)$ is the space of linear functions defined on K and $\mathcal{P}^1(K) = [\mathcal{P}^1(K)]^2$. Note that, owing to the mesh conformity, we have

$$(3.3) \quad \operatorname{trace}_{|\Sigma} \mathbf{V}_h^s = \operatorname{trace}_{|\Sigma} \mathbf{V}_h^f = \mathbf{V}_h^g.$$

In order to circumvent the lack of inf-sup stability of the pair \mathbf{V}_h^f/M_h^f , we consider the following pressure stabilized discrete bilinear form for the fluid (see, e.g., [6]):

$$a_{f,h}((\mathbf{u}_h, p_h), (\mathbf{v}_h, \theta_h)) := a_f((\mathbf{u}_h, p_h), (\mathbf{v}_h, \theta_h)) + h^2 (\nabla p_h, \nabla \theta_h)_f.$$

At last, we introduce the standard fluid-sided discrete lifting operator $\mathcal{L}_h : \mathbf{V}_h^g \rightarrow \mathbf{V}_h^f$, such that, the nodal values of $\mathcal{L}_h \boldsymbol{\mu}_h$ vanish out of Σ and $(\mathcal{L}_h \boldsymbol{\mu}_h)|_{\Sigma} = \boldsymbol{\mu}_h$, for all $\boldsymbol{\mu}_h \in \mathbf{V}_h^g$.

Algorithm 2 Fully discrete, Robin-based, loosely coupled scheme.

(1) Solid subproblem: Find $\mathbf{q}_h^{n+1}, \boldsymbol{\eta}_h^{n+1} \in \mathbf{V}_h^s$ such that $\mathbf{q}_h^{n+1/2} = \partial_{\Delta t} \boldsymbol{\eta}_h^{n+1}$ and

$$(3.4) \quad \rho_s (\partial_{\Delta t} \mathbf{q}_h^{n+1}, \boldsymbol{\xi}_h)_s + a_s(\boldsymbol{\eta}_h^{n+1/2}, \boldsymbol{\xi}_h) + \alpha \langle (\mathbf{q}_h^{n+1/2} - \mathbf{u}_h^n), \boldsymbol{\xi}_h \rangle + \langle \boldsymbol{\lambda}_h^n, \boldsymbol{\xi}_h \rangle = 0 \quad \forall \boldsymbol{\xi}_h \in \mathbf{V}_h^s.$$

(2) Fluid subproblem: Find $\mathbf{u}_h^{n+1} \in \mathbf{V}_h^f, p_h \in M_h^f$ such that

$$(3.5) \quad \rho_f (\partial_{\Delta t} \mathbf{u}_h^{n+1}, \mathbf{v}_h)_f + a_{f,h}((\mathbf{u}_h^{n+1}, p_h^{n+1}), (\mathbf{v}_h, \theta_h)) + \alpha \langle \mathbf{u}_h^{n+1} - \mathbf{q}_h^{n+1/2}, \mathbf{v}_h \rangle - \langle \boldsymbol{\lambda}_h^n, \mathbf{v}_h \rangle = 0 \quad \forall (\mathbf{v}_h, \theta_h) \in \mathbf{V}_h^f \times M_h^f.$$

(3) Energy-preserving fluid-stress evaluation: Find $\boldsymbol{\lambda}_h^{n+1} \in \mathbf{V}_h^g$ such that

$$(3.6) \quad \langle \boldsymbol{\lambda}_h^{n+1}, \boldsymbol{\mu}_h \rangle = \rho_f (\partial_{\Delta t} \mathbf{u}_h^{n+1}, \mathcal{L}_h \boldsymbol{\mu}_h)_f + a_{f,h}((\mathbf{u}_h^{n+1}, p_h^{n+1}), (\mathcal{L}_h \boldsymbol{\mu}_h, 0)) \quad \forall \boldsymbol{\mu}_h \in \mathbf{V}_h^g.$$

The proposed finite element approximation of Algorithm 1 is reported in Algorithm 2. It should be noted that the interfacial fluid stress reconstruction given by step (3) has been introduced for purely analysis purposes (see discussion below) and it should be omitted in any computer implementation. Indeed, there is no specific need of evaluating the Lagrange multiplier $\boldsymbol{\lambda}_h^{n+1}$ as an additional unknown, since the right-hand side of (3.6) can be inserted directly in (3.4) and (3.5).

Step (1) of Algorithm 2 can be reformulated as: Find $\mathbf{q}_h^{n+1}, \boldsymbol{\eta}_h^{n+1} \in \mathbf{V}_h^s$ such that

$$(3.7a) \quad \rho_s(\partial_{\Delta t} \mathbf{q}_h^{n+1}, \boldsymbol{\xi}_h)_s + a_s(\boldsymbol{\eta}_h^{n+1/2}, \boldsymbol{\xi}_h) + \alpha \langle (\partial_{\Delta t} \boldsymbol{\eta}_h^{n+1} - \mathbf{u}_h^n), \boldsymbol{\xi}_h \rangle + \langle \boldsymbol{\lambda}_h^n, \boldsymbol{\xi}_h \rangle = 0 \quad \forall \boldsymbol{\xi}_h \in \mathbf{V}_h^s,$$

$$(3.7b) \quad (\mathbf{q}_h^{n+1/2}, \boldsymbol{\phi}_h)_s - (\partial_{\Delta t} \boldsymbol{\eta}_h^{n+1}, \boldsymbol{\phi}_h)_s = 0 \quad \forall \boldsymbol{\phi}_h \in \mathbf{V}_h^s.$$

Moreover, from (3.5) and (3.6), we have that

$$(3.8) \quad \langle \boldsymbol{\lambda}_h^{n+1}, \boldsymbol{\mu}_h \rangle = \alpha \langle \mathbf{q}_h^{n+1/2} - \mathbf{u}_h^{n+1}, \boldsymbol{\mu}_h \rangle + \langle \boldsymbol{\lambda}_h^n, \boldsymbol{\mu}_h \rangle$$

for all $\boldsymbol{\mu}_h \in \mathbf{V}_h^g$. As a result, steps (2) and (3) of Algorithm 2 can be reformulated as: Find $\mathbf{u}_h^{n+1} \in \mathbf{V}_h^f, p_h \in M_h^f, \boldsymbol{\lambda}_h^{n+1} \in \mathbf{V}_h^g$ such that

$$(3.9a) \quad \rho_f(\partial_{\Delta t} \mathbf{u}_h^{n+1}, \mathbf{v}_h)_f + 2\mu(\varepsilon(\mathbf{u}_h^{n+1}), \varepsilon(\mathbf{v}_h))_f - (p_h^{n+1}, \operatorname{div} \mathbf{v}_h)_f - \langle \boldsymbol{\lambda}_h^{n+1}, \mathbf{v}_h \rangle = 0 \quad \forall \mathbf{v}_h \in \mathbf{V}_h^f$$

$$(3.9b) \quad (\operatorname{div} \mathbf{u}_h^{n+1}, \theta_h)_f + h^2(\nabla p_h^{n+1}, \nabla \theta_h)_f = 0 \quad \forall \theta_h \in M_h^f$$

$$(3.9c) \quad \alpha \langle \mathbf{u}_h^{n+1} - \mathbf{q}_h^{n+1/2}, \boldsymbol{\mu}_h \rangle + \langle \boldsymbol{\lambda}_h^{n+1} - \boldsymbol{\lambda}_h^n, \boldsymbol{\mu} \rangle = 0 \quad \forall \boldsymbol{\mu}_h \in \mathbf{V}_h^g.$$

Finally, it is also worth noting that, owing to (3.3) and (3.8), we have

$$(3.10) \quad \boldsymbol{\lambda}_h^{n+1} = \alpha(\mathbf{q}_h^{n+1/2} - \mathbf{u}_h^{n+1}) + \boldsymbol{\lambda}_h^n \quad \text{on } \Sigma$$

for $n \geq 1$. This relation, which represents discrete counterpart of (3.2)₄, is a fundamental ingredient of the stability analysis reported in next section. Also, for convenience we write the relationship:

$$(3.11) \quad \mathbf{q}_h^{n+1/2} = \partial_{\Delta t} \boldsymbol{\eta}_h^{n+1} \quad \text{on } \Omega_s.$$

3.3. Stability. Next, we will prove stability of the method. The following identity is crucial.

$$(3.12) \quad \langle \mathbf{v} - \mathbf{w}, \boldsymbol{\psi} \rangle = \frac{1}{2} \left(\|\mathbf{v}\|_{L^2(\Sigma)}^2 - \|\mathbf{w}\|_{L^2(\Sigma)}^2 + \|\boldsymbol{\psi} - \mathbf{w}\|_{L^2(\Sigma)}^2 - \|\boldsymbol{\psi} - \mathbf{v}\|_{L^2(\Sigma)}^2 \right).$$

The following quantities will allow us to state the stability result,

$$\mathfrak{S}_h^n = \|\boldsymbol{\eta}_h^n\|_S^2 + \rho_s \|\mathbf{q}_h^n\|_{L^2(\Omega_s)}^2 + \rho_f \|\mathbf{u}_h^n\|_{L^2(\Omega_f)}^2 + \Delta t (\alpha \|\mathbf{u}_h^n\|_{L^2(\Sigma)}^2 + \frac{1}{\alpha} \|\boldsymbol{\lambda}_h^n\|_{L^2(\Sigma)}^2),$$

$$\mathfrak{Z}_h^n = \rho_f \|\mathbf{u}_h^n - \mathbf{u}_h^{n-1}\|_{L^2(\Omega_f)}^2 + 2\alpha \Delta t \|\partial_{\Delta t} \boldsymbol{\eta}_h^n - \mathbf{u}_h^{n-1}\|_{L^2(\Sigma)}^2 + 4\mu \Delta t \|\varepsilon(\mathbf{u}_h^{n+1})\|_{L^2(\Omega_f)}^2 + 2h^2 \Delta t \|\nabla p_h^n\|_{L^2(\Omega_s)}^2.$$

Lemma 3.1. *Let $\{(\mathbf{q}_h^{n+1}, \boldsymbol{\eta}_h^{n+1}, \mathbf{u}_h^{n+1}, p_h^{n+1}, \boldsymbol{\lambda}_h^{n+1})\}_{n=0}^{N-1} \subset \mathbf{V}_h^s \times \mathbf{V}_h^s \times \mathbf{V}_h^f \times M_h^f \times \mathbf{V}_h^g$ be given by Algorithm 2. The following energy identity holds:*

$$\mathfrak{S}_h^M + \sum_{m=1}^M \mathfrak{Z}_h^m = \mathfrak{S}_h^0 \quad \text{for } 1 \leq M \leq N.$$

Proof. We let $\boldsymbol{\xi}_h = \mathbf{q}_h^{n+1/2}$ in (3.7a) and using (3.11) we get

$$\begin{aligned} \frac{1}{2} \|\boldsymbol{\eta}_h^{n+1}\|_S^2 + \frac{\rho_s}{2} \|\mathbf{q}_h^{n+1}\|_{L^2(\Omega_s)}^2 &= \frac{1}{2} \|\boldsymbol{\eta}_h^n\|_S^2 + \frac{\rho_s}{2} \|\mathbf{q}_h^n\|_{L^2(\Omega_s)}^2 \\ &\quad + \alpha \Delta t \langle (\mathbf{u}_h^n - \partial_{\Delta t} \boldsymbol{\eta}_h^{n+1}), \partial_{\Delta t} \boldsymbol{\eta}_h^{n+1} \rangle - \Delta t \langle \boldsymbol{\lambda}_h^n, \partial_{\Delta t} \boldsymbol{\eta}_h^{n+1} \rangle. \end{aligned}$$

If we now set $\mathbf{v}_h = \mathbf{u}_h^{n+1}$ in (3.9a) and $\theta_h = p_h^{n+1}$ in (3.9b) we obtain

$$\begin{aligned} \frac{\rho_f}{2} \|\mathbf{u}_h^{n+1}\|_{L^2(\Omega_f)}^2 + \frac{\rho_f}{2} \|\mathbf{u}_h^{n+1} - \mathbf{u}_h^n\|_{L^2(\Omega_f)}^2 + 2\mu \Delta t \|\varepsilon(\mathbf{u}_h^{n+1})\|_{L^2(\Omega_f)}^2 + h^2 \Delta t \|\nabla p_h^{n+1}\|_{L^2(\Omega_f)}^2 \\ = \frac{\rho_f}{2} \|\mathbf{u}_h^n\|_{L^2(\Omega_f)}^2 + \Delta t \langle \boldsymbol{\lambda}_h^{n+1}, \mathbf{u}_h^{n+1} \rangle. \end{aligned}$$

Adding the above two equations we get

$$\begin{aligned} & \frac{1}{2} \|\boldsymbol{\eta}_h^{n+1}\|_S^2 + \frac{\rho_s}{2} \|\mathbf{q}_h^{n+1}\|_{L^2(\Omega_s)}^2 + \frac{\rho_f}{2} \|\mathbf{u}_h^{n+1}\|_{L^2(\Omega_f)}^2 \\ & + \frac{\rho_f}{2} \|\mathbf{u}_h^{n+1} - \mathbf{u}_h^n\|_{L^2(\Omega_f)}^2 + 2\mu\Delta t \|\varepsilon(\mathbf{u}_h^{n+1})\|_{L^2(\Omega_f)}^2 + h^2\Delta t \|\nabla p_h^{n+1}\|_{L^2(\Omega_f)}^2 \\ & = \frac{1}{2} \|\boldsymbol{\eta}_h^n\|_S^2 + \frac{\rho_s}{2} \|\mathbf{q}_h^n\|_{L^2(\Omega_s)}^2 + \frac{\rho_f}{2} \|\mathbf{u}_h^n\|_{L^2(\Omega_f)}^2 + \Delta t J \end{aligned}$$

where

$$\begin{aligned} J := & \alpha \langle (\mathbf{u}_h^n - \partial_{\Delta t} \boldsymbol{\eta}_h^{n+1}), \partial_{\Delta t} \boldsymbol{\eta}_h^{n+1} \rangle - \langle \boldsymbol{\lambda}_h^n, \partial_{\Delta t} \boldsymbol{\eta}_h^{n+1} \rangle \\ & + \langle \boldsymbol{\lambda}_h^{n+1}, \mathbf{u}_h^{n+1} \rangle \end{aligned}$$

After some manipulations and using (3.10) we obtain

$$\begin{aligned} J = & \alpha \langle (\mathbf{u}_h^n - \mathbf{u}_h^{n+1} + \mathbf{u}_h^{n+1} - \partial_{\Delta t} \boldsymbol{\eta}_h^{n+1}), \partial_{\Delta t} \boldsymbol{\eta}_h^{n+1} \rangle - \langle \boldsymbol{\lambda}_h^n, \partial_{\Delta t} \boldsymbol{\eta}_h^{n+1} - \mathbf{u}_h^{n+1} + \mathbf{u}_h^{n+1} \rangle \\ & + \langle \boldsymbol{\lambda}_h^{n+1}, \mathbf{u}_h^{n+1} \rangle \\ = & \alpha \langle \mathbf{u}_h^n - \mathbf{u}_h^{n+1}, \partial_{\Delta t} \boldsymbol{\eta}_h^{n+1} \rangle + \alpha \langle \mathbf{u}_h^{n+1} - \partial_{\Delta t} \boldsymbol{\eta}_h^{n+1}, \partial_{\Delta t} \boldsymbol{\eta}_h^{n+1} \rangle \\ & - \langle \boldsymbol{\lambda}_h^n, \partial_{\Delta t} \boldsymbol{\eta}_h^{n+1} - \mathbf{u}_h^{n+1} \rangle + \langle \boldsymbol{\lambda}_h^{n+1} - \boldsymbol{\lambda}_h^n, \mathbf{u}_h^{n+1} \rangle \\ = & \alpha \langle \mathbf{u}_h^n - \mathbf{u}_h^{n+1}, \partial_{\Delta t} \boldsymbol{\eta}_h^{n+1} \rangle - \frac{1}{\alpha} \langle \boldsymbol{\lambda}_h^n, \boldsymbol{\lambda}_h^{n+1} - \boldsymbol{\lambda}_h^n \rangle \\ & + \langle \boldsymbol{\lambda}_h^{n+1} - \boldsymbol{\lambda}_h^n, \mathbf{u}_h^{n+1} - \partial_{\Delta t} \boldsymbol{\eta}_h^{n+1} \rangle. \end{aligned}$$

With (3.12), we have

$$\begin{aligned} \alpha \langle \mathbf{u}_h^n - \mathbf{u}_h^{n+1}, \partial_{\Delta t} \boldsymbol{\eta}_h^{n+1} \rangle & = \frac{\alpha}{2} \left(\|\mathbf{u}_h^n\|_{L^2(\Sigma)}^2 - \|\mathbf{u}_h^{n+1}\|_{L^2(\Sigma)}^2 \right. \\ & \quad \left. - \|\partial_{\Delta t} \boldsymbol{\eta}_h^{n+1} - \mathbf{u}_h^n\|_{L^2(\Sigma)}^2 + \|\partial_{\Delta t} \boldsymbol{\eta}_h^{n+1} - \mathbf{u}_h^{n+1}\|_{L^2(\Sigma)}^2 \right), \\ \frac{1}{\alpha} \langle \boldsymbol{\lambda}_h^n, \boldsymbol{\lambda}_h^{n+1} - \boldsymbol{\lambda}_h^n \rangle & = \frac{1}{2\alpha} \left(\|\boldsymbol{\lambda}_h^n\|_{L^2(\Sigma)}^2 - \|\boldsymbol{\lambda}_h^{n+1}\|_{L^2(\Sigma)}^2 + \|\boldsymbol{\lambda}_h^{n+1} - \boldsymbol{\lambda}_h^n\|_{L^2(\Sigma)}^2 \right). \end{aligned}$$

Using (3.10), we note that $\|\boldsymbol{\lambda}_h^{n+1} - \boldsymbol{\lambda}_h^n\|_{L^2(\Sigma)}^2 = \alpha^2 \|\partial_{\Delta t} \boldsymbol{\eta}_h^{n+1} - \mathbf{u}_h^{n+1}\|_{L^2(\Sigma)}^2$. Thus, we conclude

$$J = \frac{\alpha}{2} \left(\|\mathbf{u}_h^n\|_{L^2(\Sigma)}^2 - \|\mathbf{u}_h^{n+1}\|_{L^2(\Sigma)}^2 \right) + \frac{1}{2\alpha} \left(\|\boldsymbol{\lambda}_h^n\|_{L^2(\Sigma)}^2 - \|\boldsymbol{\lambda}_h^{n+1}\|_{L^2(\Sigma)}^2 \right) - \frac{\alpha}{2} \|\partial_{\Delta t} \boldsymbol{\eta}_h^{n+1} - \mathbf{u}_h^n\|_{L^2(\Sigma)}^2.$$

We finally arrive at

$$\frac{1}{2} \mathcal{S}_h^{n+1} + \frac{1}{2} \mathcal{Z}_h^{n+1} = \frac{1}{2} \mathcal{S}_h^n.$$

The result now follows after summing both sides. \square

4. ERROR ANALYSIS

4.1. The linear interpolant and the L^2 - projection. In order to carry out the error analysis we define the following discrete errors:

$$\begin{aligned} \mathbf{H}_h^n & := \boldsymbol{\eta}_h^n - R_h^s \boldsymbol{\eta}^n, & \mathbf{Q}_h^n & := \mathbf{q}_h^n - R_h^s \mathbf{q}^n, \\ \mathbf{U}_h^n & := \mathbf{u}_h^n - R_h^f(\mathbf{u}^n), & \boldsymbol{\Lambda}_h^n & := \boldsymbol{\lambda}_h^n - \mathbb{P}_h \boldsymbol{\lambda}^n, \\ P_h^n & := p_h^n - S_h(p^n), \end{aligned}$$

where R_h^i , $i = s, f$ are the Scott-Zhang interpolants defined in [32] projecting onto our finite element spaces V_h^s, V_h^f . Also, S_h is the Scott-Zhang interpolant into M_h^f modified by a global constant so the average on Ω_f is zero. Finally, \mathbb{P}_h is the L^2 projection onto V_h^g . Thus,

$$(4.1) \quad \langle \mathbb{P}_h \boldsymbol{\lambda}^n, \boldsymbol{\mu}_h \rangle = \langle \boldsymbol{\lambda}^n, \boldsymbol{\mu}_h \rangle, \quad \forall \boldsymbol{\mu} \in V_h^g.$$

There is flexibility in defining the Scott-Zhang interpolant and we choose the degrees of freedom on the boundary so that, $R_h^s \mathbf{v} = R_h^f \mathbf{w}$ on Σ if $\mathbf{v} \in [H^1(\Omega_s)]^2$ and $\mathbf{w} \in [H^1(\Omega_f)]^2$ and $\mathbf{v} = \mathbf{w}$ on Σ . For these interpolants, we have the well known stability result for $\mathbf{v} \in [H^1(\Omega_i)]^2$, $i = s, f$, and $r \in H^1(\Omega_f)$,

$$(4.2) \quad \|R_h^i \mathbf{v}\|_{H^1(\Omega_i)} \leq C \|\mathbf{v}\|_{H^1(\Omega_i)}, \quad \|S_h r\|_{H^1(\Omega_f)} \leq C \|r\|_{H^1(\Omega_f)}.$$

We will also need the trace inequality

$$(4.3) \quad \|\mathbf{v}\|_{L^2(\Sigma)} \leq C \|\mathbf{v}\|_{H^1(\Omega_i)}.$$

Furthermore, it is well known that for $\mathbf{v} \in [H^2(\Omega_i)]^2$, $i = s, f$, and $r \in H^2(\Omega_f)$,

$$(4.4) \quad \|R_h^i \mathbf{v} - \mathbf{v}\|_{L^2(\Omega_i)} \leq Ch^2 \|\mathbf{v}\|_{H^2(\Omega_i)}, \quad \|S_h r - r\|_{L^2(\Omega_f)} \leq Ch^2 \|r\|_{H^2(\Omega_f)},$$

$$(4.5) \quad \|R_h^i \mathbf{v} - \mathbf{v}\|_{H^1(\Omega_i)} \leq Ch \|\mathbf{v}\|_{H^2(\Omega_i)}, \quad \|S_h r - r\|_{H^1(\Omega_f)} \leq Ch \|r\|_{H^2(\Omega_f)}.$$

The interpolants restricted to the Σ will be the Scott-Zhang interpolant on Σ so we have

$$\|R_h^i \mathbf{v} - \mathbf{v}\|_{L^2(\Sigma)} + h \|R_h^i \mathbf{v} - \mathbf{v}\|_{H^1(\Sigma)} \leq Ch^2 \|\mathbf{v}\|_{H^2(\Sigma)}.$$

Thus, using the trace estimate with this approximation result we have

$$(4.6) \quad \|R_h^i \mathbf{v} - \mathbf{v}\|_{L^2(\Sigma)} + h \|R_h^i \mathbf{v} - \mathbf{v}\|_{H^1(\Sigma)} \leq Ch^2 \|\mathbf{v}\|_{H^3(\Omega_i)}, \quad \forall \mathbf{v} \in [H^3(\Omega_i)]^2.$$

We may now state consistency-type results for the solid and the fluid.

Lemma 4.1. *The following identities hold for all $\boldsymbol{\xi}_h \in \mathbf{V}_h^s$, $\mathbf{v}_h \in \mathbf{V}_h^f$, and $\boldsymbol{\mu}_h \in \mathbf{V}_h^g$.*

$$(4.7) \quad \begin{aligned} & \rho_s (\partial_{\Delta t} R_h^s \mathbf{q}^{n+1}, \boldsymbol{\xi}_h)_s + a_s (R_h^s \boldsymbol{\eta}^{n+1/2}, \boldsymbol{\xi}_h) + \alpha \langle (\partial_{\Delta t} R_h^s \boldsymbol{\eta}^{n+1} - R_h^f \mathbf{u}^n), \boldsymbol{\xi}_h \rangle + \langle \mathbb{P}_h \boldsymbol{\lambda}^n, \boldsymbol{\xi}_h \rangle \\ & = T_1(\boldsymbol{\xi}_h) + \frac{1}{2} T_2(\boldsymbol{\xi}_h) + V_1(\boldsymbol{\xi}_h) - S_2(\boldsymbol{\xi}_h) + S_3(\boldsymbol{\xi}_h), \end{aligned}$$

$$(4.8) \quad \begin{aligned} & \rho_f (\partial_{\Delta t} R_h^f \mathbf{u}^{n+1}, \mathbf{v}_h)_f + 2\mu (\varepsilon(R_h^f \mathbf{u}^{n+1}), \varepsilon(\mathbf{v}_h))_f - (S_h p^{n+1}, \operatorname{div} \mathbf{v}_h)_f - \langle \mathbb{P}_h \boldsymbol{\lambda}^{n+1}, \mathbf{v}_h \rangle = S_1(\mathbf{v}_h) + V_2(\mathbf{v}_h), \\ & (\operatorname{div} R_h^f \mathbf{u}^{n+1}, \theta_h)_f + h^2 (\nabla S_h p^{n+1}, \nabla \theta_h)_f = V_3(\theta_h) + V_4(\theta_h), \end{aligned}$$

where

$$\begin{aligned} T_1(\boldsymbol{\xi}_h) & := \rho_s (\partial_{\Delta t} R_h^s \mathbf{q}^{n+1} - \partial_t \mathbf{q}^{n+1/2}, \boldsymbol{\xi}_h)_s, \\ T_2(\boldsymbol{\xi}_h) & := \langle \boldsymbol{\lambda}^n - \boldsymbol{\lambda}^{n+1}, \boldsymbol{\xi}_h \rangle, \\ S_1(\mathbf{v}_h) & := \rho_f (\partial_{\Delta t} R_h^f \mathbf{u}^{n+1} - \partial_t R_h^f \mathbf{u}^{n+1}, \mathbf{v}_h)_f, \\ S_2(\boldsymbol{\mu}_h) & := \alpha \langle R_h^f \mathbf{u}^{n+1} - \partial_{\Delta t} R_h^s \boldsymbol{\eta}^{n+1}, \boldsymbol{\mu}_h \rangle, \\ S_3(\boldsymbol{\mu}_h) & := \alpha \langle R_h^f \mathbf{u}^{n+1} - R_h^f \mathbf{u}^n, \boldsymbol{\mu}_h \rangle, \\ V_1(\boldsymbol{\xi}_h) & := a_s (R_h^s \boldsymbol{\eta}^{n+1/2} - \boldsymbol{\eta}^{n+1/2}, \boldsymbol{\xi}_h)_s, \\ V_2(\mathbf{v}_h) & := 2\mu (\varepsilon(R_h^f \mathbf{u}^{n+1} - \mathbf{u}^{n+1}), \varepsilon(\mathbf{v}_h))_f - (S_h p^{n+1} - p^{n+1}, \operatorname{div} \mathbf{v}_h)_f, \\ V_3(\theta_h) & := (\operatorname{div} (R_h^f \mathbf{u}^{n+1} - \mathbf{u}^{n+1}), \theta_h)_f, \\ V_4(\theta_h) & := h^2 (\nabla S_h p^{n+1}, \nabla \theta_h)_f. \end{aligned}$$

Proof. For (4.7), let \mathbb{L}_1 denote the left-hand side. Then we have

$$\begin{aligned}
\mathbb{L}_1 &= \rho_s(\partial_{\Delta t} R_h^s \mathbf{q}^{n+1} - \partial_t \mathbf{q}^{n+1/2}, \boldsymbol{\xi}_h)_s + \rho_s(\partial_t \mathbf{q}^{n+1/2}, \boldsymbol{\xi}_h)_s + a_s(R_h^s \boldsymbol{\eta}^{n+1/2}, \boldsymbol{\xi}_h) \\
&\quad + \alpha \langle (\partial_{\Delta t} R_h^s \boldsymbol{\eta}^{n+1} - R_h^f \mathbf{u}^{n+1}), \boldsymbol{\xi}_h \rangle + S_3(\boldsymbol{\xi}_h) + \langle \boldsymbol{\lambda}^n, \boldsymbol{\xi}_h \rangle \\
&= T_1(\boldsymbol{\xi}_h) - a_s(\boldsymbol{\eta}^{n+1/2}, \boldsymbol{\xi}_h) + a_s(R_h^s \boldsymbol{\eta}^{n+1/2}, \boldsymbol{\xi}_h) - \langle \boldsymbol{\lambda}^{n+1/2}, \boldsymbol{\xi}_h \rangle \\
&\quad - S_2(\boldsymbol{\xi}_h) + S_3(\boldsymbol{\xi}_h) + \langle \boldsymbol{\lambda}^n, \boldsymbol{\xi}_h \rangle \\
&= T_1(\boldsymbol{\xi}_h) + V_1(\boldsymbol{\xi}_h) + \frac{1}{2} T_2(\boldsymbol{\xi}_h) - S_2(\boldsymbol{\xi}_h) + S_3(\boldsymbol{\xi}_h).
\end{aligned}$$

For (4.8), let \mathbb{L}_2 denote the left hand side. We have

$$\begin{aligned}
\mathbb{L}_2 &= \rho_f(\partial_{\Delta t} R_h^f \mathbf{u}^{n+1} - \partial_t \mathbf{u}^{n+1}, \mathbf{v}_h)_f + \rho_f(\partial_t \mathbf{u}^{n+1}, \mathbf{v}_h)_f \\
&\quad + 2\mu(\varepsilon(R_h^f \mathbf{u}^{n+1}), \varepsilon(\mathbf{v}_h))_f - (S_h p^{n+1}, \operatorname{div} \mathbf{v}_h)_f - \langle \boldsymbol{\lambda}^{n+1}, \mathbf{v}_h \rangle \\
&= S_1(\mathbf{v}_h) - 2\mu(\varepsilon(\mathbf{u}^{n+1}), \varepsilon(\mathbf{v}_h))_f + (p^{n+1}, \operatorname{div} \mathbf{v}_h)_f + \langle \boldsymbol{\lambda}^{n+1}, \mathbf{v}_h \rangle \\
&\quad + 2\mu(\varepsilon(R_h^f \mathbf{u}^{n+1}), \varepsilon(\mathbf{v}_h))_f - (S_h p^{n+1}, \operatorname{div} \mathbf{v}_h)_f - \langle \boldsymbol{\lambda}^{n+1}, \mathbf{v}_h \rangle \\
&= S_1(\mathbf{v}_h) + V_2(\mathbf{v}_h).
\end{aligned}$$

Recall that $\operatorname{div} \mathbf{u}^n = 0$ for all $n \geq 1$. For (4.9), let \mathbb{L}_3 denote the left hand side. We have

$$\begin{aligned}
\mathbb{L}_3 &= (\operatorname{div} R_h^f \mathbf{u}^{n+1}, \theta_h)_f + h^2(\nabla S_h p^{n+1}, \nabla \theta_h)_f \\
&= (\operatorname{div} R_h^f \mathbf{u}^{n+1} - \operatorname{div} \mathbf{u}^{n+1}, \theta_h)_f + h^2(\nabla S_h p^{n+1}, \nabla \theta_h)_f \\
&= V_3(\theta_h) + V_4(\theta_h).
\end{aligned}$$

□

From Lemma 4.1, we find that the following error equations follow immediately after applying (3.7) and (3.9).

Corollary 4.2. *For all $\boldsymbol{\xi}_h \in \mathbf{V}_h^s$, $\mathbf{v}_h \in \mathbf{V}_h^f$, and $\theta_h \in M_h^f$, the following identities hold.*

$$\begin{aligned}
&\rho_s(\partial_{\Delta t} \mathbf{Q}_h^{n+1}, \boldsymbol{\xi}_h)_s + a_s(\mathbf{H}_h^{n+1/2}, \boldsymbol{\xi}_h) + \alpha \langle (\partial_{\Delta t} \mathbf{H}_h^{n+1/2} - \mathbf{U}_h^n), \boldsymbol{\xi}_h \rangle + \langle \boldsymbol{\Lambda}_h^n, \boldsymbol{\xi}_h \rangle \\
(4.10) \quad &= -T_1(\boldsymbol{\xi}_h) - \frac{1}{2} T_2(\boldsymbol{\xi}_h) - V_1(\boldsymbol{\xi}_h) + S_2(\boldsymbol{\xi}_h) - S_3(\boldsymbol{\xi}_h),
\end{aligned}$$

(4.11)

$$\rho_f(\partial_{\Delta t} \mathbf{U}_h^{n+1}, \mathbf{v}_h)_f + 2\mu(\varepsilon(\mathbf{U}_h^{n+1}), \varepsilon(\mathbf{v}_h))_f - (P_h^{n+1}, \operatorname{div} \mathbf{v}_h)_f - \langle \boldsymbol{\Lambda}_h^{n+1}, \mathbf{v}_h \rangle = -S_1(\mathbf{v}_h) - V_2(\mathbf{v}_h),$$

(4.12)

$$(\operatorname{div} \mathbf{U}_h^{n+1}, \theta_h)_f + h^2(\nabla P_h^{n+1}, \nabla \theta_h)_f = -V_3(\theta_h) - V_4(\theta_h).$$

We also will need the following identities.

Lemma 4.3. *The following identities hold:*

$$(4.13a) \quad \boldsymbol{\Lambda}_h^{n+1} - \boldsymbol{\Lambda}_h^n = \alpha(\partial_{\Delta t} \mathbf{H}_h^{n+1} - \mathbf{U}_h^{n+1}) + \mathbf{g}_1^{n+1}$$

$$(4.13b) \quad \mathbf{Q}_h^{n+1/2} = \partial_{\Delta t} \mathbf{H}_h^{n+1} - R_h^s \mathbf{g}_2^{n+1},$$

where

$$\begin{aligned}
\mathbf{g}_1^{n+1} &:= \alpha(\partial_{\Delta t} R_h^s \boldsymbol{\eta}^{n+1} - R_h^f \mathbf{u}^{n+1}) - (\mathbb{P}_h \boldsymbol{\lambda}^{n+1} - \mathbb{P}_h \boldsymbol{\lambda}^n), \\
\mathbf{g}_2^{n+1} &:= \mathbf{q}^{n+1/2} - \partial_{\Delta t} \boldsymbol{\eta}^{n+1}.
\end{aligned}$$

Proof. Using (3.10) we obtain

$$\begin{aligned}\mathbf{\Lambda}_h^{n+1} - \mathbf{\Lambda}_h^n &= (\boldsymbol{\lambda}_h^{n+1} - \boldsymbol{\lambda}_h^n) - (\mathbb{P}_h \boldsymbol{\lambda}^{n+1} - \mathbb{P}_h \boldsymbol{\lambda}^n) \\ &= \alpha(\partial_{\Delta t} \boldsymbol{\eta}_h^{n+1} - \mathbf{u}_h^{n+1}) - (\mathbb{P}_h \boldsymbol{\lambda}^{n+1} - \mathbb{P}_h \boldsymbol{\lambda}^n) \\ &= \alpha(\partial_{\Delta t} \mathbf{H}_h^{n+1} - \mathbf{U}_h^{n+1}) + \mathbf{g}_1^{n+1}.\end{aligned}$$

We also have by (3.7b)

$$\begin{aligned}\mathbf{q}_h^{n+1/2} &= \mathbf{q}_h^{n+1} - R_h^s \mathbf{q}^{n+1/2} \\ &= \partial_{\Delta t} \mathbf{H}_h^{n+1} + \partial_{\Delta t} R_h^s \boldsymbol{\eta}^{n+1} - R_h^s \mathbf{q}^{n+1/2} \\ &= \partial_{\Delta t} \mathbf{H}_h^{n+1} - R_h^s \mathbf{g}_2^{n+1}.\end{aligned}$$

□

4.2. Approximation Results. Finally, before we prove error estimates we will prove approximation inequalities. We recall the definition of space-time norms where X is a Hilbert space

$$\|\mathbf{v}\|_{L^2(r_1, r_2; X)}^2 := \int_{r_1}^{r_2} \|\mathbf{v}(\cdot, s)\|_X^2 ds.$$

The following are a series of approximation estimates. The proofs are elementary and appear in the appendix for completeness.

Lemma 4.4. *The following inequalities hold*

(4.14a)

$$\|\partial_{\Delta t} R_h^s \mathbf{q}^{n+1} - \partial_t \mathbf{q}^{n+1/2}\|_{L^2(\Omega_s)}^2 \leq C \left(\frac{h^4}{\Delta t} \|\partial_t \mathbf{q}\|_{L^2(t_n, t_{n+1}; H^2(\Omega_s))}^2 + \Delta t^3 \|\partial_t^3 \mathbf{q}\|_{L^2(t_n, t_{n+1}; L^2(\Omega_s))}^2 \right),$$

$$(4.14b) \quad \|\boldsymbol{\lambda}^{n+1} - \boldsymbol{\lambda}^n\|_{L^2(\Sigma)}^2 \leq C \Delta t \left(\mu^2 \|\partial_t \mathbf{u}\|_{L^2(t_n, t_{n+1}; H^2(\Omega_f))}^2 + \|\partial_t p\|_{L^2(t_n, t_{n+1}; H^1(\Omega_f))}^2 \right),$$

$$(4.14c) \quad \|R_h^f \mathbf{u}^{n+1} - R_h^f \mathbf{u}^n\|_{L^2(\Sigma)}^2 \leq C \Delta t \|\partial_t \mathbf{u}\|_{L^2(t_n, t_{n+1}; H^1(\Omega_f))}^2,$$

$$(4.14d) \quad \|R_h^s \mathbf{g}_2^{n+1}\|_{L^2(\Sigma)}^2 \leq C \Delta t^3 \|\partial_t^3 \boldsymbol{\eta}\|_{L^2(t_n, t_{n+1}; H^1(\Omega_s))}^2,$$

(4.14e)

$$\|\partial_{\Delta t} R_h^f \mathbf{u}^{n+1} - \partial_t \mathbf{u}^{n+1}\|_{L^2(\Omega_f)}^2 \leq C \left(\frac{h^4}{\Delta t} \|\partial_t \mathbf{u}\|_{L^2(t_n, t_{n+1}; H^2(\Omega_f))}^2 + \Delta t \|\partial_t^2 \mathbf{u}\|_{L^2(t_n, t_{n+1}; L^2(\Omega_f))}^2 \right),$$

$$(4.14f) \quad \|\nabla R_h^s \mathbf{g}_2^{n+1}\|_{L^2(\Omega_s)}^2 \leq C \Delta t^3 \|\partial_t^3 \boldsymbol{\eta}\|_{L^2(t_n, t_{n+1}; H^1(\Omega_s))}^2,$$

$$(4.14g) \quad \|\mathbf{g}_1^{n+1}\|_{L^2(\Sigma)}^2 \leq C \Delta t \left(\mu^2 \|\partial_t \mathbf{u}\|_{L^2(t_n, t_{n+1}; H^2(\Omega_f))}^2 + \|\partial_t p\|_{L^2(t_n, t_{n+1}; H^1(\Omega_f))}^2 + \alpha^2 \|\partial_t^2 \boldsymbol{\eta}\|_{L^2(t_n, t_{n+1}; H^1(\Omega_f))}^2 \right),$$

$$(4.14h) \quad \|S_h p^{n+1} - p^{n+1}\|_{L^2(\Omega_f)}^2 \leq C \left(\Delta t h^4 \|\partial_t p\|_{L^2(t_n, t_{n+1}; H^2(\Omega_f))}^2 + \frac{h^4}{\Delta t} \|p\|_{L^2(t_n, t_{n+1}; H^2(\Omega_f))}^2 \right),$$

$$(4.14i) \quad \|\varepsilon(R_h^f \mathbf{u}^{n+1} - \mathbf{u}^{n+1})\|_{L^2(\Omega_f)}^2 \leq C \left(\Delta t h^2 \|\partial_t \mathbf{u}\|_{L^2(t_n, t_{n+1}; H^2(\Omega_f))}^2 + \frac{h^2}{\Delta t} \|\mathbf{u}\|_{L^2(t_n, t_{n+1}; H^2(\Omega_f))}^2 \right),$$

$$(4.14j) \quad \|\nabla S_h p^{n+1}\|_{L^2(\Omega_f)}^2 \leq C \left(\Delta t \|\partial_t p\|_{L^2(t_n, t_{n+1}; H^1(\Omega_f))}^2 + \frac{1}{\Delta t} \|p\|_{L^2(t_n, t_{n+1}; H^1(\Omega_f))}^2 \right),$$

$$(4.14k) \quad \|\mathbf{u}^{n+1}\|_{H^3(\Omega_f)}^2 \leq C \left(\Delta t \|\partial_t \mathbf{u}\|_{L^2(t_n, t_{n+1}; H^3(\Omega_f))}^2 + \frac{1}{\Delta t} \|\mathbf{u}\|_{L^2(t_n, t_{n+1}; H^3(\Omega_f))}^2 \right),$$

(4.14l)

$$\|\nabla(R_h^s \boldsymbol{\eta}^{n+1/2} - \boldsymbol{\eta}^{n+1/2})\|_{L^2(\Omega_s)}^2 \leq C \left(h^2 \Delta t \|\partial_t \boldsymbol{\eta}\|_{L^2(t_n, t_{n+1}; H^2(\Omega_s))}^2 + \frac{h^2}{\Delta t} \|\boldsymbol{\eta}\|_{L^2(t_n, t_{n+1}; H^2(\Omega_s))}^2 \right),$$

$$(4.14m) \quad \|\nabla(R_h^s - I) \partial_{\Delta t} \boldsymbol{\eta}^{n+1}\|_{L^2(\Omega_s)}^2 \leq C \frac{h^2}{\Delta t} \|\partial_t \boldsymbol{\eta}\|_{L^2(t_n, t_{n+1}; H^2(\Omega_s))}^2.$$

4.3. **Main Theorem.** Now we can prove the main error estimate. We define the following quantities:

$$\begin{aligned} \mathcal{S}_h^n &:= \|\mathbf{H}_h^n\|_S^2 + \rho_s \|\mathbf{Q}_h^n\|_{L^2(\Omega_s)}^2 + \rho_f \|\mathbf{U}_h^n\|_{L^2(\Omega_f)}^2, \\ \mathcal{E}_h^n &:= \Delta t \alpha \|\mathbf{U}_h^n\|_{L^2(\Sigma)}^2 + \frac{\Delta t}{\alpha} \|\boldsymbol{\Lambda}_h^n\|_{L^2(\Sigma)}^2, \\ \mathcal{W}_h^n &:= \rho_f \|\mathbf{U}_h^n - \mathbf{U}_h^{n-1}\|_{L^2(\Omega_f)}^2 + 4\mu \Delta t \|\varepsilon(\mathbf{U}_h^n)\|_{L^2(\Omega_f)}^2 + 2\Delta t h^2 \|\nabla P_h^n\|_{L^2(\Omega_s)}^2, \\ \mathcal{Z}_h^n &:= \Delta t \alpha \|\partial_{\Delta t} \mathbf{H}_h^n - \mathbf{U}_h^{n-1}\|_{L^2(\Sigma)}^2. \end{aligned}$$

Theorem 4.5. Let $(\mathbf{u}, \boldsymbol{\lambda}, \boldsymbol{\eta}, \mathbf{q})$ be a regular enough solution of (2.4) and let $\{(\boldsymbol{\eta}_h^n, \mathbf{q}_h^n, \mathbf{u}_h^n, p_h^n, \boldsymbol{\lambda}_h^n)\}_{n=1}^N$ be given by Algorithm 2. The following discrete error estimate holds:

$$\max_{1 \leq m \leq N} (\mathcal{S}_h^m + \mathcal{E}_h^m) + \sum_{m=1}^N (\mathcal{W}_h^m + \mathcal{Z}_h^m) \leq 4(\mathcal{S}_h^0 + \mathcal{E}_h^0) + CY\Psi,$$

where

$$\begin{aligned} Y &:= \left(\frac{T}{\alpha} (\mu^2 + 1) + \alpha T \right) \Delta t + \left(\frac{1}{\alpha} (\mu^2 + 1) + \rho_f T + \alpha \right) \Delta t^2 \\ &\quad + T \alpha \Delta t^3 + \left(T(\rho_s + 1) + \alpha + 1 \right) \Delta t^4 + \left(T + 1 + \alpha \right) h^2 \\ &\quad + \left(T(\rho_f + \rho_s) + \frac{1}{\mu} \right) h^4 + (1 + \mu) h^2 \Delta t^2 + \frac{h^4 \Delta t^2}{\mu}, \end{aligned}$$

and

$$\begin{aligned} \Psi &:= \|\partial_t \boldsymbol{\eta}\|_{L^2(0, T; H^2(\Omega_s))}^2 + \|\partial_t^2 \boldsymbol{\eta}\|_{L^2(0, T; H^2(\Omega_s))}^2 + \|\partial_t^3 \boldsymbol{\eta}\|_{L^2(0, T; H^1(\Omega_s))}^2 + \|\partial_t^4 \boldsymbol{\eta}\|_{L^2(0, T; L^2(\Omega_s))}^2 \\ &\quad + \|\mathbf{u}\|_{L^2(0, T; H^3(\Omega_f))}^2 + \|\partial_t \mathbf{u}\|_{L^2(0, T; H^2(\Omega_f))}^2 + \|\partial_t^2 \mathbf{u}\|_{L^2(0, T; L^2(\Omega_f))}^2 + \|p\|_{L^2(0, T; H^1(\Omega_f))}^2 \\ &\quad + \|\partial_t p\|_{L^2(0, T; H^1(\Omega_f))}^2 + \|\boldsymbol{\eta}\|_{L^\infty(0, T; H^2(\Omega_s))}^2. \end{aligned}$$

Proof. Using (4.13b) we have

$$a_s(\mathbf{H}_h^{n+1/2}, \mathbf{Q}_h^{n+1/2}) = \frac{1}{2\Delta t} \|\mathbf{H}_h^{n+1}\|_S^2 - \frac{1}{2\Delta t} \|\mathbf{H}_h^n\|_S^2 - a_s(\mathbf{H}_h^{n+1/2}, R_h^s \mathbf{g}_2^{n+1}).$$

If we let $\boldsymbol{\xi}_h = \mathbf{Q}_h^{n+1/2}$ in (4.10) we obtain

$$\begin{aligned} (4.15) \quad & \frac{1}{2} \|\mathbf{H}_h^{n+1}\|_S^2 + \frac{\rho_s}{2} \|\mathbf{Q}_h^{n+1}\|_{L^2(\Omega_s)}^2 \\ &= \frac{1}{2} \|\mathbf{H}_h^n\|_S^2 + \frac{\rho_s}{2} \|\mathbf{Q}_h^n\|_{L^2(\Omega_s)}^2 + \Delta t a_s(\mathbf{H}_h^{n+1/2}, R_h^s \mathbf{g}_2^{n+1}) - \Delta t T_1(\mathbf{Q}_h^{n+1/2}) \\ &\quad - \frac{\Delta t}{2} T_2(\mathbf{Q}_h^{n+1/2}) - \Delta t V_1(\mathbf{Q}_h^{n+1/2}) + \Delta t S_2(\mathbf{Q}_h^{n+1/2}) - \Delta t S_3(\mathbf{Q}_h^{n+1/2}) + J_1, \end{aligned}$$

where

$$J_1 := -\alpha \Delta t \langle (\partial_{\Delta t} \mathbf{H}_h^{n+1} - \mathbf{U}_h^n), \mathbf{Q}_h^{n+1/2} \rangle - \Delta t \langle \boldsymbol{\Lambda}_h^n, \mathbf{Q}_h^{n+1/2} \rangle.$$

We simplify J_1 by using (4.13a)

$$\begin{aligned} J_1 &= -\alpha\Delta t\langle(\partial_{\Delta t}\mathbf{H}_h^{n+1} - \mathbf{U}_h^{n+1}), \mathbf{Q}_h^{n+1/2}\rangle + \Delta t\langle\Lambda_h^{n+1} - \Lambda_h^n, \mathbf{Q}_h^{n+1/2}\rangle \\ &\quad - \alpha\Delta t\langle\mathbf{U}_h^{n+1} - \mathbf{U}_h^n, \mathbf{Q}_h^{n+1/2}\rangle - \Delta t\langle\Lambda_h^{n+1}, \mathbf{Q}_h^{n+1/2}\rangle \\ &= \Delta t\langle\mathbf{g}_1^{n+1}, \mathbf{Q}_h^{n+1/2}\rangle - \alpha\Delta t\langle\mathbf{U}_h^{n+1} - \mathbf{U}_h^n, \mathbf{Q}_h^{n+1/2}\rangle - \Delta t\langle\Lambda_h^{n+1}, \mathbf{Q}_h^{n+1/2}\rangle. \end{aligned}$$

Therefore, if we plug this in to (4.15) we have

$$\begin{aligned} &\frac{1}{2}\|\mathbf{H}_h^{n+1}\|_S^2 + \frac{\rho_s}{2}\|\mathbf{Q}_h^{n+1}\|_{L^2(\Omega_s)}^2 \\ &= \frac{1}{2}\|\mathbf{H}_h^n\|_S^2 + \frac{\rho_s}{2}\|\mathbf{Q}_h^n\|_{L^2(\Omega_s)}^2 + \Delta ta_s(\mathbf{H}_h^{n+1/2}, R_h\mathbf{g}_2^{n+1}) - \Delta tT_1(\mathbf{Q}_h^{n+1/2}) \\ &\quad - \frac{\Delta t}{2}T_2(\mathbf{Q}_h^{n+1/2}) - \Delta tV_1(\boldsymbol{\xi}_h) + \Delta tS_2(\mathbf{Q}_h^{n+1/2}) - \Delta tS_3(\mathbf{Q}_h^{n+1/2}) \\ (4.16) \quad &+ \Delta t\langle\mathbf{g}_1^{n+1}, \mathbf{Q}_h^{n+1/2}\rangle - \alpha\Delta t\langle\mathbf{U}_h^{n+1} - \mathbf{U}_h^n, \mathbf{Q}_h^{n+1/2}\rangle - \Delta t\langle\Lambda_h^{n+1}, \mathbf{Q}_h^{n+1/2}\rangle. \end{aligned}$$

If we now set $\mathbf{v}_h = \mathbf{U}_h^{n+1}$ in (4.11) and $\theta_h = P_h^{n+1}$ in (4.12) we get

$$\begin{aligned} &\frac{\rho_f}{2}\|\mathbf{U}_h^{n+1}\|_{L^2(\Omega_f)}^2 + \frac{\rho_f}{2}\|\mathbf{U}_h^{n+1} - \mathbf{U}_h^n\|_{L^2(\Omega_f)}^2 + \Delta t2\mu\|\varepsilon(\mathbf{U}_h^{n+1})\|_{L^2(\Omega_f)}^2 + \Delta th^2\|\nabla P_h^{n+1}\|_{L^2(\Omega_s)}^2 \\ (4.17) \quad &= \frac{1}{2}\|\mathbf{U}_h^n\|_{L^2(\Omega_f)}^2 + \Delta t\langle\Lambda_h^{n+1}, \mathbf{U}_h^{n+1}\rangle - \Delta tS_1(\mathbf{U}_h^{n+1}) - \Delta tV_2(\mathbf{U}_h) - \Delta tV_3(P_h) - \Delta tV_4(P_h). \end{aligned}$$

If we use that

$$-\Delta tS_3(\mathbf{Q}_h^{n+1/2}) - \frac{\Delta t}{2}T_2(\mathbf{Q}_h^{n+1/2}) + \Delta t\langle\mathbf{g}_1^{n+1}, \mathbf{Q}_h^{n+1/2}\rangle = \frac{\Delta t}{2}T_2(\mathbf{Q}_h^{n+1/2})$$

and add (4.16) and (4.17), we may write the following

$$(4.18) \quad \frac{1}{2}\mathcal{S}_h^{n+1} + \frac{1}{2}\mathcal{W}_h^{n+1} = \frac{1}{2}\mathcal{S}_h^n + K_1 + \dots + K_9 + J_2,$$

where

$$\begin{aligned} K_1 &:= -\Delta tT_1(\mathbf{Q}_h^{n+1/2}), & K_2 &:= \frac{\Delta t}{2}T_2(\mathbf{Q}_h^{n+1/2}), & K_3 &:= -\Delta tS_3(\mathbf{Q}_h^{n+1/2}), \\ K_4 &:= -\Delta tS_1(\mathbf{U}_h^{n+1}), & K_5 &:= \Delta ta_s(\mathbf{H}_h^{n+1/2}, R_h^s\mathbf{g}_2^{n+1}), & K_6 &:= -\Delta tV_3(P_h^{n+1}), \\ K_7 &:= -\Delta tV_4(P_h^{n+1}), & K_8 &:= -\Delta tV_1(\mathbf{Q}_h^{n+1/2}), & K_9 &:= -\Delta tV_2(\mathbf{U}_h^{n+1}). \end{aligned}$$

and

$$J_2 := -\alpha\Delta t\langle\mathbf{U}_h^{n+1} - \mathbf{U}_h^n, \mathbf{Q}_h^{n+1/2}\rangle - \Delta t\langle\Lambda_h^{n+1}, \mathbf{Q}_h^{n+1/2}\rangle + \Delta t\langle\Lambda_h^{n+1}, \mathbf{U}_h^{n+1}\rangle.$$

Using (4.13b) we see that

$$\begin{aligned} J_2 &= -\alpha\Delta t\langle\mathbf{U}_h^{n+1} - \mathbf{U}_h^n, \partial_{\Delta t}\mathbf{H}_h^{n+1}\rangle - \Delta t\langle\Lambda_h^{n+1}, \partial_{\Delta t}\mathbf{H}_h^{n+1} - \mathbf{U}_h^{n+1}\rangle \\ &\quad + \alpha\Delta t\langle\mathbf{U}_h^{n+1} - \mathbf{U}_h^n, R_h^s\mathbf{g}_2^{n+1}\rangle + \Delta t\langle\Lambda_h^{n+1}, R_h^s\mathbf{g}_2^{n+1}\rangle. \end{aligned}$$

Using (4.13a) gives

$$\begin{aligned} J_2 &= -\alpha\Delta t\langle\mathbf{U}_h^{n+1} - \mathbf{U}_h^n, \partial_{\Delta t}\mathbf{H}_h^{n+1}\rangle - \frac{\Delta t}{\alpha}\langle\Lambda_h^{n+1}, \Lambda_h^{n+1} - \Lambda_h^n\rangle, \\ &\quad + \alpha\Delta t\langle\mathbf{U}_h^{n+1} - \mathbf{U}_h^n, R_h^s\mathbf{g}_2^{n+1}\rangle + \Delta t\langle\Lambda_h^{n+1}, R_h^s\mathbf{g}_2^{n+1} + \frac{\mathbf{g}_1^{n+1}}{\alpha}\rangle. \end{aligned}$$

We can then use (3.12) to get

$$\begin{aligned} -\alpha\Delta t\langle \mathbf{U}_h^{n+1} - \mathbf{U}_h^n, \partial_{\Delta t}\mathbf{H}_h^{n+1} \rangle &= -\frac{\alpha\Delta t}{2}(\|\mathbf{U}_h^{n+1}\|_{L^2(\Sigma)}^2 - \|\mathbf{U}_h^n\|_{L^2(\Sigma)}^2) \\ &\quad - \frac{\alpha\Delta t}{2}(\|\partial_{\Delta t}\mathbf{H}_h^{n+1} - \mathbf{U}_h^n\|_{L^2(\Sigma)}^2 - \|\partial_{\Delta t}\mathbf{H}_h^{n+1} - \mathbf{U}_h^{n+1}\|_{L^2(\Sigma)}^2). \\ -\frac{\Delta t}{\alpha}\langle \mathbf{\Lambda}_h^{n+1}, \mathbf{\Lambda}_h^{n+1} - \mathbf{\Lambda}_h^n \rangle &= -\frac{\Delta t}{2\alpha}(\|\mathbf{\Lambda}_h^{n+1}\|_{L^2(\Sigma)}^2 - \|\mathbf{\Lambda}_h^n\|_{L^2(\Sigma)}^2 + \|\mathbf{\Lambda}_h^{n+1} - \mathbf{\Lambda}_h^n\|_{L^2(\Sigma)}^2). \end{aligned}$$

Next, we note from (4.13a) that we have

$$\begin{aligned} \frac{1}{2\alpha}\|\mathbf{\Lambda}_h^{n+1} - \mathbf{\Lambda}_h^n\|_{L^2(\Sigma)}^2 &= \frac{\alpha}{2}\|\partial_{\Delta t}\mathbf{H}_h^{n+1} - \mathbf{U}_h^{n+1}\|_{L^2(\Sigma)}^2 + \frac{1}{2\alpha}\|\mathbf{g}_1^{n+1}\|_{L^2(\Sigma)}^2 \\ &\quad + \langle \partial_{\Delta t}\mathbf{H}_h^{n+1} - \mathbf{U}_h^{n+1}, \mathbf{g}_1^{n+1} \rangle + \langle \mathbf{U}_h^{n+1} - \mathbf{U}_h^n, \mathbf{g}_1^{n+1} \rangle. \end{aligned}$$

Therefore, combining the above equations we have

$$\begin{aligned} J_2 &:= -\frac{\alpha\Delta t}{2}(\|\mathbf{U}_h^{n+1}\|_{L^2(\Sigma)}^2 - \|\mathbf{U}_h^n\|_{L^2(\Sigma)}^2 + \|\partial_{\Delta t}\mathbf{H}_h^{n+1} - \mathbf{U}_h^n\|_{L^2(\Sigma)}^2) \\ &\quad - \frac{\Delta t}{2\alpha}(\|\mathbf{\Lambda}_h^{n+1}\|_{L^2(\Sigma)}^2 - \|\mathbf{\Lambda}_h^n\|_{L^2(\Sigma)}^2) - \frac{\Delta t}{2\alpha}\|\mathbf{g}_1^{n+1}\|_{L^2(\Sigma)}^2 - \Delta t\langle \partial_{\Delta t}\mathbf{H}_h^{n+1} - \mathbf{U}_h^n, \mathbf{g}_1^{n+1} \rangle \\ &\quad + \Delta t\langle \mathbf{\Lambda}_h^{n+1}, R_h^s\mathbf{g}_2^{n+1} + \frac{\mathbf{g}_1^{n+1}}{\alpha} \rangle + \Delta t\langle \mathbf{U}_h^{n+1} - \mathbf{U}_h^n, \alpha R_h^s\mathbf{g}_2^{n+1} + \mathbf{g}_1^{n+1} \rangle. \end{aligned}$$

Substituting this into (4.18) we arrive at

$$\begin{aligned} (4.19) \quad &\frac{1}{2}\mathcal{S}_h^{n+1} + \frac{1}{2}\mathcal{E}_h^{n+1} + \frac{1}{2}\mathcal{W}_h^{n+1} + \frac{1}{2}\mathcal{Z}_h^{n+1} + \frac{\Delta t}{2\alpha}\|\mathbf{g}_1^{n+1}\|_{L^2(\Sigma)}^2 \\ &= \frac{1}{2}\mathcal{S}_h^n + \frac{1}{2}\mathcal{E}_h^n + \sum_{i=1}^{12} K_i, \end{aligned}$$

where

$$\begin{aligned} K_{10} &:= -\Delta t\langle \partial_{\Delta t}\mathbf{H}_h^{n+1} - \mathbf{U}_h^n, \mathbf{g}_1^{n+1} \rangle, \quad K_{11} := \Delta t\langle \mathbf{\Lambda}_h^{n+1}, R_h^s\mathbf{g}_2^{n+1} + \frac{\mathbf{g}_1^{n+1}}{\alpha} \rangle, \\ K_{12} &:= \Delta t\langle \mathbf{U}_h^{n+1} - \mathbf{U}_h^n, \alpha R_h^s\mathbf{g}_2^{n+1} + \mathbf{g}_1^{n+1} \rangle. \end{aligned}$$

Before proceeding to bound all the terms, we apply (4.13b) to K_8 and obtain

$$K_8 = -\Delta ta_s((R_h^s - I)\boldsymbol{\eta}^{n+1/2}, \partial_{\Delta t}\mathbf{H}_h^{n+1}) + \Delta ta_s((R_h^s - I)\boldsymbol{\eta}^{n+1/2}, R_h^s\mathbf{g}_2^{n+1}).$$

One can verify the following discrete integration by parts

$$-\Delta ta_s((R_h^s - I)\boldsymbol{\eta}^{n+1/2}, \partial_{\Delta t}\mathbf{H}_h^{n+1}) = B^{n+1} + \Delta ta_s((R_h^s - I)\partial_{\Delta t}\boldsymbol{\eta}^{n+1}, \mathbf{H}_h^{n+1/2}).$$

where

$$B^{n+1} := a_s((R_h^s - I)\boldsymbol{\eta}^n, \mathbf{H}_h^n) - a_s((R_h^s - I)\boldsymbol{\eta}^{n+1}, \mathbf{H}_h^{n+1}).$$

Thus, we have

$$K_8 = B^{n+1} + \Delta ta_s((R_h^s - I)\partial_{\Delta t}\boldsymbol{\eta}^{n+1}, \mathbf{H}_h^{n+1/2}) + \Delta ta_s((R_h^s - I)\boldsymbol{\eta}^{n+1/2}, R_h^s\mathbf{g}_2^{n+1}).$$

Now we bound each K_i for $1 \leq i \leq 12$. The number $\delta > 0$ would be chosen sufficiently small later. Using the Cauchy-Schwarz inequality we get

$$K_1 \leq \Delta t\|\partial_{\Delta t}R_h^s\mathbf{q}^{n+1} - \partial_t\mathbf{q}^{n+1/2}\|_{L^2(\Omega_s)}\|\mathbf{Q}_h^{n+1/2}\|_{L^2(\Omega_s)}.$$

If we apply the geometric-arithmetic mean inequality we get

$$K_1 \leq \delta\frac{\rho_s\Delta t}{T}(\|\mathbf{Q}_h^{n+1}\|_{L^2(\Omega_s)}^2 + \|\mathbf{Q}_h^n\|_{L^2(\Omega_s)}^2) + C(\delta)T\Delta t\rho_s\|\partial_{\Delta t}R_h^s\mathbf{q}^{n+1} - \partial_t\mathbf{q}^{n+1/2}\|_{L^2(\Omega_s)}^2.$$

To bound K_2 we use (4.13b)

$$K_2 = -\frac{\Delta t}{2}(T_2(\partial_{\Delta t}\mathbf{H}_h^{n+1} - \mathbf{U}_h^n) + T_2(\mathbf{U}_h^n) + T_2(R_h^s \mathbf{g}_2^{n+1})).$$

Therefore, after using the Cauchy-Schwarz inequality we have

$$K_2 \leq \frac{\Delta t}{2} \|\boldsymbol{\lambda}^{n+1} - \boldsymbol{\lambda}^n\|_{L^2(\Sigma)} (\|\partial_{\Delta t}\mathbf{H}_h^{n+1} - \mathbf{U}_h^n\|_{L^2(\Sigma)} + \|\mathbf{U}_h^n\|_{L^2(\Sigma)} + \|R_h^s \mathbf{g}_2^{n+1}\|_{L^2(\Sigma)}).$$

Hence, using the geometric-arithmetic mean inequality we see that

$$\begin{aligned} K_2 &\leq \delta \left(\frac{\Delta t^2 \alpha}{T} \|\mathbf{U}_h^n\|_{L^2(\Sigma)}^2 + \Delta t \alpha \|\partial_{\Delta t}\mathbf{H}_h^{n+1} - \mathbf{U}_h^n\|_{L^2(\Sigma)}^2 \right) \\ &\quad + \frac{C(\delta)}{\alpha} (\Delta t + T) \|\boldsymbol{\lambda}^{n+1} - \boldsymbol{\lambda}^n\|_{L^2(\Sigma)}^2 + C(\delta) \alpha \Delta t \|R_h^s \mathbf{g}_2^{n+1}\|_{L^2(\Sigma)}^2. \end{aligned}$$

Similarly, we have

$$K_3 \leq \Delta t \alpha \|R_h^f \mathbf{u}^{n+1} - R_h^f \mathbf{u}^n\|_{L^2(\Sigma)} (\|\partial_{\Delta t}\mathbf{H}_h^{n+1} - \mathbf{U}_h^n\|_{L^2(\Sigma)} + \|\mathbf{U}_h^n\|_{L^2(\Sigma)} + \|R_h^s \mathbf{g}_2^{n+1}\|_{L^2(\Sigma)}),$$

and

$$\begin{aligned} K_3 &\leq \delta \left(\frac{\Delta t^2 \alpha}{T} \|\mathbf{U}_h^n\|_{L^2(\Sigma)}^2 + \Delta t \alpha \|\partial_{\Delta t}\mathbf{H}_h^{n+1} - \mathbf{U}_h^n\|_{L^2(\Sigma)}^2 \right) \\ &\quad + C(\delta) \alpha (\Delta t + T) \|R_h^f \mathbf{u}^{n+1} - R_h^f \mathbf{u}^n\|_{L^2(\Sigma)}^2 + C(\delta) \alpha \Delta t \|R_h^s \mathbf{g}_2^{n+1}\|_{L^2(\Sigma)}^2. \end{aligned}$$

Following this same process, we have

$$\begin{aligned} K_4 &\leq \delta \frac{\rho_f \Delta t}{T} \|\mathbf{U}_h^{n+1}\|_{L^2(\Omega_f)}^2 + C(\delta) \rho_f \Delta t T \|\partial_{\Delta t} R_h^f \mathbf{u}^{n+1} - \partial_t \mathbf{u}^{n+1}\|_{L^2(\Omega_f)}^2, \\ K_5 &\leq \delta \frac{\Delta t}{T} (\|\mathbf{H}_h^{n+1}\|_S^2 + \|\mathbf{H}_h^n\|_S^2) + C(\delta) T \Delta t \|R_h^s \mathbf{g}_2^{n+1}\|_S^2, \\ K_7 &\leq \delta \Delta t h^2 \|\nabla P_h^{n+1}\|_{L^2(\Omega_f)}^2 + C(\delta) \Delta t h^2 \|\nabla S_h p^{n+1}\|_{L^2(\Omega_f)}^2, \\ K_8 &\leq \delta \frac{\Delta t}{T} (\|\mathbf{H}_h^n\|_S^2 + \|\mathbf{H}_h^{n+1}\|_S^2) + C \Delta t \|R_h^s \mathbf{g}_2^{n+1}\|_S^2 \\ &\quad + C(\delta) \Delta t T \|(R_h^s - I) \partial_{\Delta t} \boldsymbol{\eta}^{n+1}\|_S^2 + C \Delta t \|(R_h^s - I) \boldsymbol{\eta}^{n+1/2}\|_S^2 + B^{n+1}, \\ K_{10} &\leq \delta \alpha \Delta t \|\partial_{\Delta t} \mathbf{H}_h^{n+1} - \mathbf{U}_h^n\|_{L^2(\Sigma)}^2 + \frac{C(\delta) \Delta t}{\alpha} \|\mathbf{g}_1^{n+1}\|_{L^2(\Sigma)}^2, \\ K_{11} &\leq \delta \frac{(\Delta t)^2}{T \alpha} \|\boldsymbol{\Lambda}_h^{n+1}\|_{L^2(\Sigma)}^2 + \frac{C(\delta) T}{\alpha} \|\alpha R_h^s \mathbf{g}_2^{n+1} + \mathbf{g}_1^{n+1}\|_{L^2(\Sigma)}^2, \\ K_{12} &\leq \delta \frac{(\Delta t)^2 \alpha}{T} (\|\mathbf{U}_h^{n+1}\|_{L^2(\Sigma)}^2 + \|\mathbf{U}_h^n\|_{L^2(\Sigma)}^2) + \frac{C(\delta) T}{\alpha} \|\alpha R_h^s \mathbf{g}_2^{n+1} + \mathbf{g}_1^{n+1}\|_{L^2(\Sigma)}^2. \end{aligned}$$

To estimate K_6 , we perform integration by parts and proceed as before. Thus,

$$\begin{aligned} K_6 &= \Delta t (R_h^f \mathbf{u}^{n+1} - \mathbf{u}^{n+1}, \nabla P_h^{n+1})_f - \Delta t \langle (R_h^f \mathbf{u}^{n+1} - \mathbf{u}^{n+1}) \cdot \mathbf{n}, P_h^{n+1} \rangle \\ &\leq \Delta t \|R_h^f \mathbf{u}^{n+1} - \mathbf{u}^{n+1}\|_{L^2(\Omega_f)} \|\nabla P_h\|_{L^2(\Omega_f)} + \Delta t \|R_h^f \mathbf{u}^{n+1} - \mathbf{u}^{n+1}\|_{L^2(\Sigma)} \|P_h^{n+1}\|_{L^2(\Sigma)} \\ &\leq C \Delta t h^2 \|\mathbf{u}^{n+1}\|_{H^2(\Omega_f)} \|\nabla P_h^{n+1}\|_{L^2(\Omega_f)} + C \Delta t h^2 \|\mathbf{u}^{n+1}\|_{H^3(\Omega_f)} \|\nabla P_h^{n+1}\|_{L^2(\Omega_f)}, \end{aligned}$$

where the last step follows from applying (4.6) and using the trace inequality (4.3) on P_h^{n+1} . We also used Poincaré's inequality. Thus, applying this result along with Young's inequality, we have

$$K_6 \leq \delta \Delta t h^2 \|\nabla P_h^{n+1}\|_{L^2(\Omega_f)}^2 + C(\delta) \Delta t h^2 \|\mathbf{u}^{n+1}\|_{H^3(\Omega_f)}^2.$$

Finally, for K_9 , we can easily show that

$$K_9 \leq \delta \Delta t \mu \|\varepsilon(\mathbf{U}_h^{n+1})\|_{L^2(\Omega_f)}^2 + C(\delta) \Delta t \mu \|\varepsilon(R_h^f \mathbf{u}^{n+1} - \mathbf{u}^{n+1})\|_{L^2(\Omega_f)}^2 + C(\delta) \frac{\Delta t}{\mu} \|S_h p^{n+1} - p^{n+1}\|_{L^2(\Omega_f)}^2.$$

Combining the above inequalities, we have

$$\sum_{1 \leq i \leq 12} K_i \leq 12\delta \frac{\Delta t}{T} (\mathcal{S}_h^{n+1} + \mathcal{S}_h^n + \mathcal{E}_h^{n+1} + \mathcal{E}_h^n) + 12\delta (\mathcal{Z}_h^{n+1} + \mathcal{W}_h^{n+1}) + C(\delta)G^{n+1} + B^{n+1},$$

where $G^{n+1} := \sum_{i=1}^{14} G_i^{n+1}$ such that

$$\begin{aligned} G_1^{n+1} &:= T\Delta t \rho_s \|\partial_{\Delta t} R_h^s \mathbf{q}^{n+1} - \partial_t \mathbf{q}^{n+1/2}\|_{L^2(\Omega_s)}^2, & G_2^{n+1} &:= \frac{1}{\alpha} (\Delta t + T) \|\boldsymbol{\lambda}^{n+1} - \boldsymbol{\lambda}^n\|_{L^2(\Sigma)}^2, \\ G_3^{n+1} &:= \alpha (\Delta t + T) \|R_h^f \mathbf{u}^{n+1} - R_h^f \mathbf{u}^n\|_{L^2(\Sigma)}^2, & G_4^{n+1} &:= \Delta t \alpha \|R_h^s \mathbf{g}_2^{n+1}\|_{L^2(\Sigma)}^2, \\ G_5^{n+1} &:= \rho_f \Delta t T \|\partial_{\Delta t} R_h^f \mathbf{u}^{n+1} - \partial_t \mathbf{u}^{n+1}\|_{L^2(\Omega_f)}^2, & G_6^{n+1} &:= (\Delta t + T\Delta t) \|R_h^s \mathbf{g}_2^{n+1}\|_S^2, \\ G_7^{n+1} &:= \frac{\Delta t}{\alpha} \|\mathbf{g}_1^{n+1}\|_{L^2(\Sigma)}^2, & G_8^{n+1} &:= \frac{T}{\alpha} \|\alpha R_h^s \mathbf{g}_2^{n+1} + \mathbf{g}_1^{n+1}\|_{L^2(\Sigma)}^2, \\ G_9^{n+1} &:= \frac{\Delta t}{\mu} \|S_h p^{n+1} - p^{n+1}\|_{L^2(\Omega_f)}^2, & G_{10}^{n+1} &:= \mu \Delta t \|\varepsilon (R_h^f \mathbf{u}^{n+1} - \mathbf{u}^{n+1})\|_{L^2(\Omega_f)}^2, \\ G_{11}^{n+1} &:= \Delta t h^2 \|\nabla S_h p^{n+1}\|_{L^2(\Omega_f)}^2, & G_{12}^{n+1} &:= \Delta t h^2 \|\mathbf{u}^{n+1}\|_{H^3(\Omega_f)}^2, \\ G_{13}^{n+1} &:= \Delta t \|(R_h^s - I) \boldsymbol{\eta}^{n+1/2}\|_S^2, & G_{14}^{n+1} &:= \Delta t T \|(R_h^s - I) \partial_{\Delta t} \boldsymbol{\eta}^{n+1}\|_S^2. \end{aligned}$$

Therefore, if we take the sum of (4.19) from 1 to $M \leq N$, we have

$$(4.20) \quad \frac{1}{2} (\mathcal{S}_h^M + \mathcal{E}_h^M) + \frac{1}{2} \sum_{m=1}^M (\mathcal{W}_h^m + \mathcal{Z}_h^m) \leq \frac{1}{2} (\mathcal{S}_h^0 + \mathcal{E}_h^0) + 24\delta \max_{0 \leq m \leq N} \left(\frac{1}{2} \mathcal{S}_h^m + \frac{1}{2} \mathcal{E}_h^m \right) + 12\delta \sum_{m=1}^M (\mathcal{W}_h^m + \mathcal{Z}_h^m) + \sum_{m=1}^M B^m + C(\delta) \sum_{m=1}^M G^m.$$

We can use the telescoping sum to get

$$\sum_{m=1}^M B^m = a_s((R_h^s - I) \boldsymbol{\eta}^0, \mathbf{H}_h^0) - a_s((R_h^s - I) \boldsymbol{\eta}^M, \mathbf{H}_h^M).$$

We may then bound this term using Cauchy-Schwartz and Young's inequality, giving us

$$\sum_{m=1}^M B^m \leq \delta (\|\mathbf{H}_h^M\|_S^2 + \|\mathbf{H}_h^0\|_S^2) + C(\delta) (\|(R_h - I) \boldsymbol{\eta}^M\|_S^2 + \|(R_h - I) \boldsymbol{\eta}^0\|_S^2).$$

If we take δ small enough, say $24\delta \leq 1/2$, we obtain after using (4.20)

$$(4.21) \quad \frac{1}{4} \max_{1 \leq m \leq N} (\mathcal{S}_h^m + \mathcal{E}_h^m) + \frac{1}{4} \sum_{m=1}^N (\mathcal{W}_h^m + \mathcal{Z}_h^m) \leq \mathcal{S}_h^0 + \mathcal{E}_h^0 + C \max_{0 \leq m \leq N} \|(R_h - I) \boldsymbol{\eta}^m\|_S^2 + C \sum_{m=1}^N G^m.$$

Now we proceed to bound $\sum_{m=1}^N G_i^m$ for every $1 \leq i \leq 14$. Using (4.14a) we have

$$\sum_{m=1}^N G_1^m \leq CT \rho_s \left(h^4 \|\partial_t \mathbf{q}\|_{L^2(0,T;H^2(\Omega_s))}^2 + \Delta t^4 \|\partial_t^3 \mathbf{q}\|_{L^2(0,T;L^2(\Omega_s))}^2 \right).$$

Using (4.14b) we get

$$\sum_{m=1}^N G_2^m \leq C \left(\frac{1}{\alpha} (\Delta t + T) \right) \Delta t \left(\mu^2 \|\partial_t \mathbf{u}\|_{L^2(0,T;H^2(\Omega_f))}^2 + \|\partial_t p\|_{L^2(0,T;H^1(\Omega_f))}^2 \right).$$

If we apply (4.14c) we obtain

$$\sum_{m=1}^N G_3^m \leq C\alpha(\Delta t + T)\Delta t \|\partial_t \mathbf{u}\|_{L^2(0,T;H^1(\Omega_f))}^2.$$

From (4.14d), it follows that

$$\sum_{m=1}^N G_4^m \leq C\Delta t^4 \alpha \|\partial_t^3 \boldsymbol{\eta}\|_{L^2(0,T;H^1(\Omega_s))}^2.$$

We can use (4.14e) to obtain

$$\sum_{m=1}^N G_5^m \leq CT\rho_f \left(h^4 \|\partial_t \mathbf{u}\|_{L^2(0,T;H^2(\Omega_f))}^2 + \Delta t^2 \|\partial_t^2 \mathbf{u}\|_{L^2(0,T;L^2(\Omega_f))}^2 \right).$$

As a result of (4.14f) and (4.14g) we have

$$\begin{aligned} \sum_{m=1}^N G_6^m &\leq C(1+T)\Delta t^4 \|\partial_t^3 \boldsymbol{\eta}\|_{L^2(0,T;H^2(\Omega_s))}^2, \\ \sum_{m=1}^N G_7^m &\leq C \frac{\Delta t^2}{\alpha} \left(\mu^2 \|\partial_t \mathbf{u}\|_{L^2(0,T;H^2(\Omega_f))}^2 + \|\partial_t p\|_{L^2(0,T;H^1(\Omega_f))}^2 + \alpha^2 \|\partial_t^2 \boldsymbol{\eta}\|_{L^2(0,T;H^1(\Omega_f))}^2 \right), \\ \sum_{m=1}^N G_8^m &\leq CT\Delta t^3 \alpha \|\partial_t^3 \boldsymbol{\eta}\|_{L^2(0,T;H^1(\Omega_s))}^2 \\ &\quad + C \frac{\Delta t T}{\alpha} \left(\mu^2 \|\partial_t \mathbf{u}\|_{L^2(0,T;H^2(\Omega_f))}^2 + \|\partial_t p\|_{L^2(t_n, t_{n+1}; H^1(\Omega_f))}^2 + \alpha^2 \|\partial_t^2 \boldsymbol{\eta}\|_{L^2(0,T;H^1(\Omega_f))}^2 \right). \end{aligned}$$

Proceeding in the same manner, from (4.14h) - (4.14m) we have

$$\begin{aligned} \sum_{m=1}^N G_9^m &\leq C \frac{h^4}{\mu} \left(\Delta t^2 \|\partial_t p\|_{L^2(0,T;H^2(\Omega_f))}^2 + h^4 \|p\|_{L^2(0,T;H^2(\Omega_f))}^2 \right), \\ \sum_{m=1}^N G_{10}^m &\leq C\mu \left(\Delta t^2 h^2 \|\partial_t \mathbf{u}\|_{L^2(0,T;H^2(\Omega_f))}^2 + h^2 \|\mathbf{u}\|_{L^2(0,T;H^2(\Omega_f))}^2 \right), \\ \sum_{m=1}^N G_{11}^m &\leq Ch^2 \left(\Delta t^2 \|\partial_t p\|_{L^2(0,T;H^2(\Omega_f))}^2 + \|p\|_{L^2(0,T;H^2(\Omega_f))}^2 \right), \\ \sum_{m=1}^N G_{12}^m &\leq Ch^2(\Delta t^2 + 1) \|\mathbf{u}^{n+1}\|_{L^2(0,T;H^3(\Omega_f))}^2, \\ \sum_{m=1}^N G_{13}^m &\leq Ch^2 \left(\Delta t^2 \|\partial_t \boldsymbol{\eta}\|_{L^2(0,T;H^2(\Omega_s))}^2 + \|\boldsymbol{\eta}\|_{L^2(0,T;H^2(\Omega_s))}^2 \right), \\ \sum_{m=1}^N G_{14}^m &\leq Ch^2 T \|\partial_t \boldsymbol{\eta}\|_{L^2(0,T;H^2(\Omega_s))}^2. \end{aligned}$$

We can also have the bound

$$\max_{0 \leq m \leq N} \|(R_h - I)\boldsymbol{\eta}^m\|_S^2 \leq Ch^2 \max_{0 \leq m \leq N} \|\boldsymbol{\eta}(t_m)\|_{H^2(\Omega_s)}^2 \leq Ch^2 \|\boldsymbol{\eta}\|_{L^\infty(0,T;H^2(\Omega_s))}^2.$$

Thus, combining the terms we get

$$\max_{0 \leq m \leq N} \|(R_h - I)\boldsymbol{\eta}^m\|_S^2 + \sum_{m=1}^N G^m \leq CY\Psi.$$

Plugging this into (4.21) completes the proof. \square

5. NUMERICAL EXPERIMENTS

The purpose of this section is to illustrate, via numerical experiments, the performance of the loosely coupled scheme given by Algorithm 2. We consider the well-known pressure wave propagation example (see, e.g., [17, Section 6.1.1]). In (2.1)-(2.3), we have $\Omega_f = [0, L] \times [0, R]$, $\Omega_s = [0, L] \times [R, R + \epsilon]$, $\Sigma = [0, L] \times \{R\}$, $L = 6$, $R = 0.5$ and $\epsilon = 0.1$. All the units are given in the CGS system. At the left fluid boundary $x = 0$ we impose a sinusoidal pressure of maximal amplitude 2×10^4 during 5×10^{-3} s, corresponding to half a period. Free traction is enforced at $x = L$ and a symmetry condition on the bottom wall. Transverse membrane effects in the solid are included through a zeroth-order term $c_0 \boldsymbol{\eta}$ in $(2.2)_1$. Zero displacement and zero traction are respectively enforced on the solid later and upper boundaries. The fluid physical parameters are $\rho^f = 1$ and $\mu = 0.035$. For the solid we have $\rho^s = 1.1$, $L_1 = 1.15 \cdot 10^6$, $L_2 = 1.7 \cdot 10^6$ and $c_0 = 4 \cdot 10^6$. A multiplying coefficient of $10^{-3}/\mu$ is applied to the Brezzi-Pitkäranta pressure stabilization method. All the simulations have been performed with **FreeFem++** (see [27]).

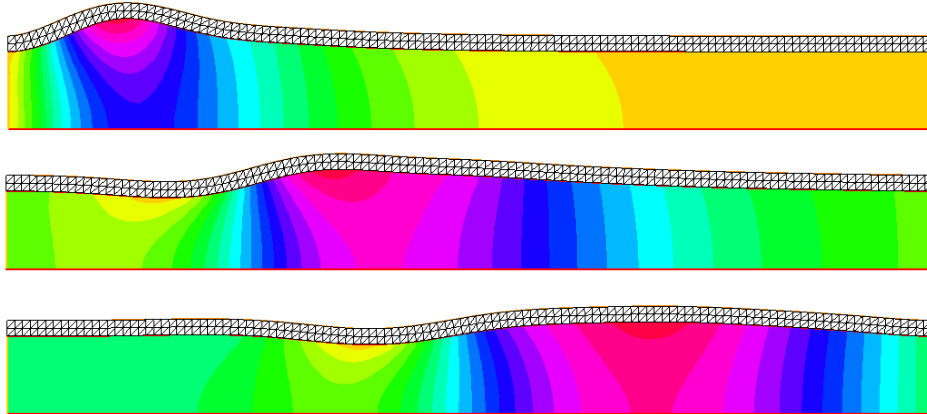


FIGURE 1. Snapshots of the fluid pressure and solid deformation at $t = 5 \cdot 10^{-3}$, 10^{-2} and $1.5 \cdot 10^{-2}$ (from top to bottom). Algorithm 2 with $\tau = 2.5 \cdot 10^{-4}$, $h = 0.05$ and $\alpha = 500$.

Figure 1 shows some snapshots of the fluid pressure approximation obtained with Algorithm 2 for $\tau = 2.5 \cdot 10^{-4}$, $h = 0.05$ and $\alpha = 500$. For illustration purposes, the fluid and solid domains are displayed in deformed configuration (magnified by a factor 5). The numerical solution remains stable, in agreement with Lemma 3.1, and shows a propagating pressure-wave.

5.1. Accuracy. In order to assess the accuracy of Algorithm 2, a reference solution has been generated using a strongly coupled scheme and a high space-time grid resolution ($h = 3.125 \cdot 10^{-3}$, $\Delta t = 10^{-6}$). Convergence histories are measured in terms of the relative elastic energy-norm $\|\boldsymbol{\eta}_{ref}^N - \boldsymbol{\eta}_h^N\|_S$ at time $t = 0.015$, by refining both in time and in space at the same rate, namely, by taking

$$(\Delta t, h) \in \left\{ \left(\frac{5 \cdot 10^{-4}}{2^i}, \frac{10^{-1}}{2^i} \right) \right\}_{i=0}^4.$$

This allows, in particular, to highlight the h -uniformity of the error estimate provided in Theorem 4.5.

Figure 2 reports the corresponding convergence histories obtained with Algorithm 2 with $\alpha = 500$ and the strongly coupled scheme. We can clearly see that Algorithm 2 delivers an overall sub-optimal convergence rate, close to $\mathcal{O}(\sqrt{h})$. This is in agreement with the error estimate provided

by Theorem 4.5 with $\Delta t = \mathcal{O}(h)$. The strongly coupled scheme yields an overall $\mathcal{O}(h)$ accuracy, as expected.

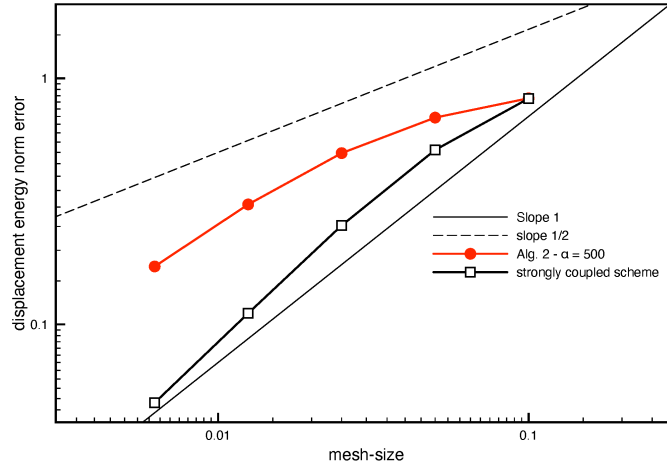


FIGURE 2. Time-convergence history of the displacement at $t = 0.015$, with $\Delta t = \mathcal{O}(h)$ obtained with Algorithm 2 ($\alpha = 500$) and the strongly coupled scheme.

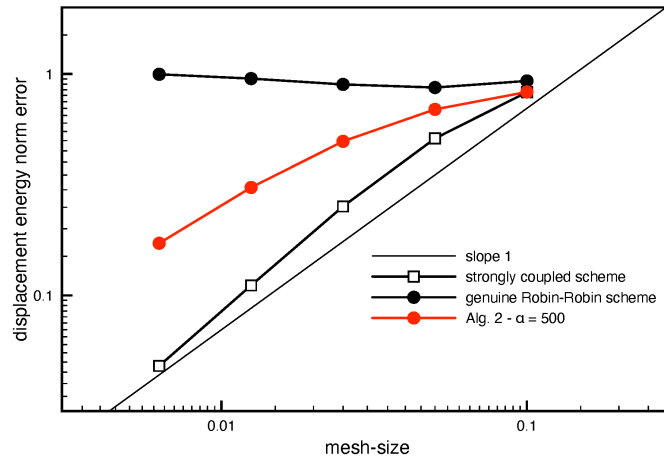


FIGURE 3. Time-convergence history of the displacement at $t = 0.015$, with $\Delta t = \mathcal{O}(h)$ obtained with Algorithm 2 ($\alpha = 500$), the strongly coupled scheme and the genuine Robin-Robin explicit coupling scheme from [13, Algorithm 4].

Another salient feature of Figure 2 is that it highlights the h -uniformity of the time-splitting error. This is indeed one of the key features of Algorithm 2 with respect to the genuine Robin-Robin explicit coupling scheme reported in [13, Algorithm 4], in which $\alpha = \gamma\mu/h$. The resulting splitting error scales as $\mathcal{O}(\Delta t/h)$, and hence preventing convergence under $\Delta t = \mathcal{O}(h)$. Figure 3 provides numerical evidence of this issue and shows Algorithm 2 fixes it.

The h -uniformity of the splitting error has further implications in terms of accuracy. Indeed, owing to Theorem 4.5, one correction iteration in Algorithm 2 should be enough to achieve overall $\mathcal{O}(h)$

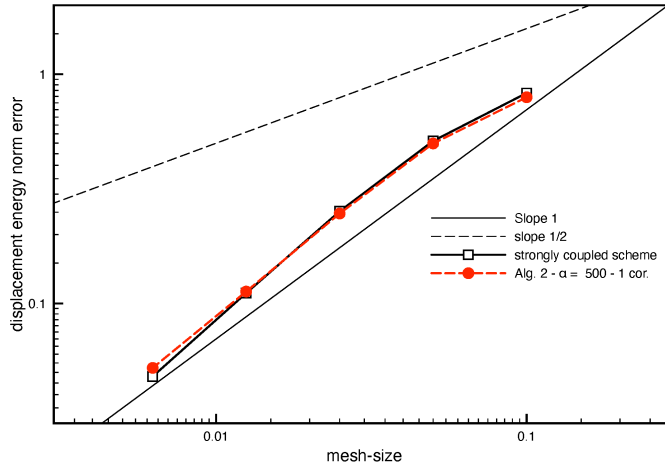


FIGURE 4. Time-convergence history of the displacement at $t = 0.015$, with $\Delta t = \mathcal{O}(h)$ obtained with the strongly coupled scheme and Algorithm 2 with 1 correction iteration ($\alpha = 500$).

accuracy, under $\Delta t = \mathcal{O}(h)$. Numerical evidence of this is given in Figure 4. We can also notice that the convergence behavior is very close to the one provided by the strongly coupled scheme. This is a fundamental advantage of Algorithm 2 with respect to the genuine Robin-Robin explicit coupling scheme, in which both high order extrapolation and several corrections are need to cope with the loss of h -uniformity (see [13]).

The superior accuracy of the Algorithm 2 with one correction iteration is also clearly visible in Figure 5, where the interface displacements associated to Figures 2 and 4 (first four points of each curve) are displayed. For comparison purposes, the reference displacement is also shown. Observe that the defect-correction variant of Algorithm 2 retrieves the accuracy of the strongly coupled scheme.

5.2. Impact of the Robin coefficient α . We now turn our attention to another fundamental question related to Algorithm 2: the choice of the Robin parameter α . From Theorem 4.5, the leading term of the time splitting error scales as

$$\sqrt{\alpha^{-1} + \alpha} \sqrt{\Delta t}.$$

We can hence anticipate that accuracy should be spoiled for (relatively) large or small values of α . Numerical evidence of this behavior is provided in Figures 6 and 7, where the convergence histories obtained with Algorithm 2 (without and with correction) are reported for different values of α . Indeed, the best accuracy is obtained for (relatively) moderate values of α , ranging from 250 to 2000, whereas out of this interval accuracy degrades rapidly. It should be noted that, since α is not dimensionless, these optimal values are expected to depend on the physical parameters of the system.

REFERENCES

- [1] M. Astorino, F. Chouly, and M. A. Fernández. Robin based semi-implicit coupling in fluid-structure interaction: stability analysis and numerics. *SIAM J. Sci. Comput.*, 31(6):4041–4065, 2009/10.
- [2] S. Badia, F. Nobile, and C. Vergara. Fluid–structure partitioned procedures based on robin transmission conditions. *Journal of Computational Physics*, 227(14):7027–7051, 2008.
- [3] S. Badia, A. Quaini, and A. Quarteroni. Splitting methods based on algebraic factorization for fluid-structure interaction. *SIAM J. Sci. Comput.*, 30(4):1778–1805, 2008.
- [4] J. W. Banks, W. D. Henshaw, and D. W. Schwendeman. An analysis of a new stable partitioned algorithm for FSI problems. Part I: Incompressible flow and elastic solids. *J. Comput. Phys.*, 269:108–137, 2014.

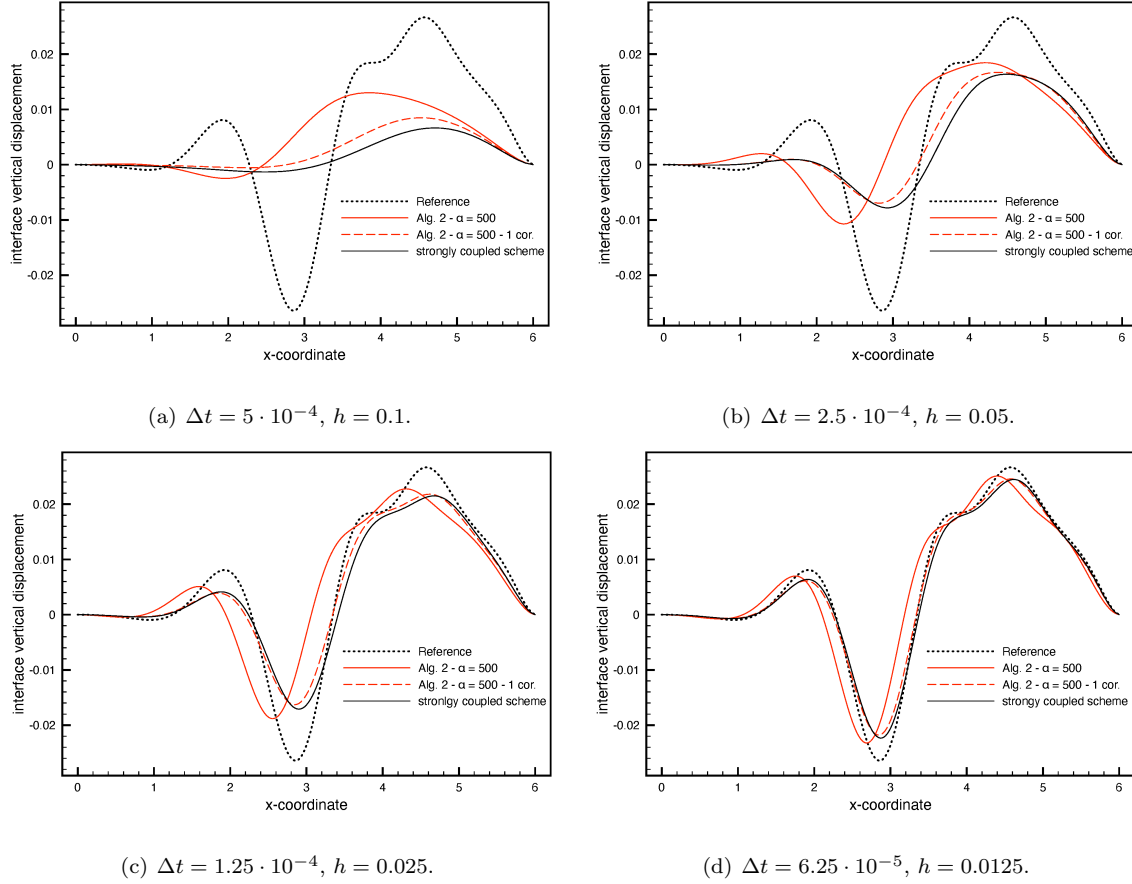


FIGURE 5. Comparison of the displacements at $t = 0.015$ obtained for different levels of space-time refinement, $\Delta t = \mathcal{O}(h)$.

- [5] S. Brenner and R. Scott. *The mathematical theory of finite element methods*, volume 15. Springer Science & Business Media, 2007.
- [6] F. Brezzi and J. Pitkäranta. On the stabilization of finite element approximations of the Stokes equations. In *Efficient solutions of elliptic systems (Kiel, 1984)*, volume 10 of *Notes Numer. Fluid Mech.*, pages 11–19. Vieweg, 1984.
- [7] M. Bukač and B. Muha. Stability and convergence analysis of the extensions of the kinematically coupled scheme for the fluid-structure interaction. *SIAM J. Numer. Anal.*, 54(5):3032–3061, 2016.
- [8] M. Bukač, S. Čanić, R. Glowinski, B. Muha, and A. Quaini. A modular, operator-splitting scheme for fluid-structure interaction problems with thick structures. *Internat. J. Numer. Methods Fluids*, 74(8):577–604, 2014.
- [9] M. Bukač, S. Čanić, and B. Muha. A partitioned scheme for fluid-composite structure interaction problems. *J. Comput. Phys.*, 281:493–517, 2015.
- [10] M. Bukač, I. Yotov, and P. Zunino. An operator splitting approach for the interaction between a fluid and a multilayered poroelastic structure. *Numer. Methods Partial Differential Equations*, 31(4):1054–1100, 2015.
- [11] E. Burman, R. Durst, and J. Guzman. Stability and error analysis of a splitting method using Robin-Robin coupling applied to a fluid-structure interaction problem. *arXiv e-prints*, page arXiv:1911.06760, Nov. 2019.
- [12] E. Burman and M. A. Fernández. Stabilization of explicit coupling in fluid-structure interaction involving fluid incompressibility. *Computer Methods in Applied Mechanics and Engineering*, 198(5-8):766–784, 2009.
- [13] E. Burman and M. A. Fernández. Explicit strategies for incompressible fluid-structure interaction problems: Nitsche type mortaring versus robin-robin coupling. *International Journal for Numerical Methods in Engineering*, 97(10):739–758, 2014.
- [14] P. Causin, J.-F. Gerbeau, and F. Nobile. Added-mass effect in the design of partitioned algorithms for fluid-structure problems. *Computer methods in applied mechanics and engineering*, 194(42-44):4506–4527, 2005.

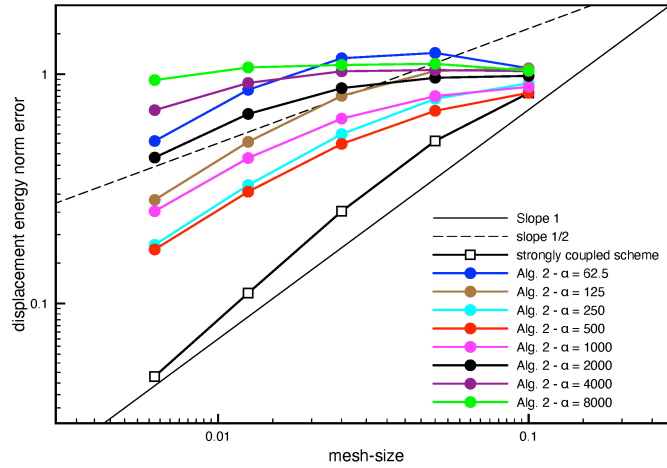


FIGURE 6. Time-convergence history of the displacement at $t = 0.015$, with $\Delta t = \mathcal{O}(h)$ obtained with Algorithm 2 for different values of α .

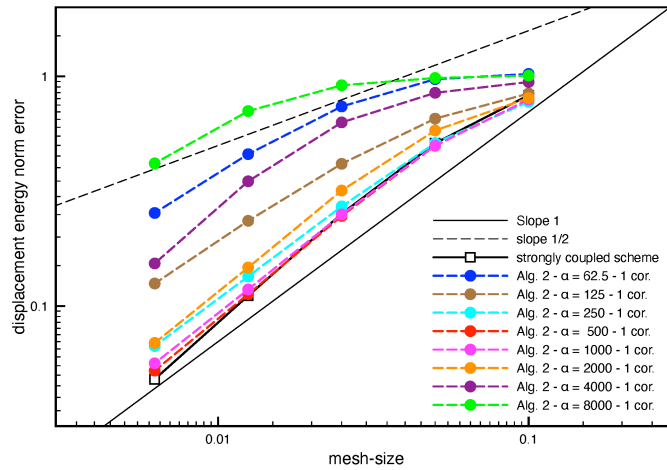


FIGURE 7. Time-convergence history of the displacement at $t = 0.015$, with $\Delta t = \mathcal{O}(h)$ obtained with Algorithm 2 with 1 correction iteration for different values of α .

- [15] C. Farhat, M. Lesoinne, and P. LeTallec. Load and motion transfer algorithms for fluid/structure interaction problems with non-matching discrete interfaces: momentum and energy conservation, optimal discretization and application to aeroelasticity. *Comput. Methods Appl. Mech. Engrg.*, 157(1-2):95–114, 1998.
- [16] M. Fernández, J. Mullaert, and M. Vidrascu. Explicit Robin-Neumann schemes for the coupling of incompressible fluids with thin-walled structures. *Comput. Methods Appl. Mech. Engrg.*, 267:566–593, 2013.
- [17] M. Fernández, J. Mullaert, and M. Vidrascu. Generalized Robin-Neumann explicit coupling schemes for incompressible fluid-structure interaction: stability analysis and numerics. *Internat. J. Numer. Methods Engrg.*, 101(3):199–229, 2015.
- [18] M. A. Fernández. Incremental displacement-correction schemes for incompressible fluid-structure interaction. *Numer. Math.*, 123(1):21–65, 2013.
- [19] M. A. Fernández, J.-F. Gerbeau, and C. Grandmont. A projection semi-implicit scheme for the coupling of an elastic structure with an incompressible fluid. *Internat. J. Numer. Methods Engrg.*, 69(4):794–821, 2007.
- [20] M. A. Fernández, M. Landajueta, and M. Vidrascu. Fully decoupled time-marching schemes for incompressible fluid/thin-walled structure interaction. *J. Comput. Phys.*, 297:156–181, 2015.

- [21] M. A. Fernández and J. Mullaert. Convergence and error analysis for a class of splitting schemes in incompressible fluid-structure interaction. *IMA J. Numer. Anal.*, 36(4):1748–1782, 2016.
- [22] M. A. Fernández, J. Mullaert, and M. Vidrascu. Generalized robin–neumann explicit coupling schemes for incompressible fluid-structure interaction: Stability analysis and numerics. *International Journal for Numerical Methods in Engineering*, 101(3):199–229, 2015.
- [23] C. Förster, W. A. Wall, and E. Ramm. Artificial added mass instabilities in sequential staggered coupling of nonlinear structures and incompressible viscous flows. *Comput. Methods Appl. Mech. Engrg.*, 196(7):1278–1293, 2007.
- [24] L. Gerardo-Giorda, F. Nobile, and C. Vergara. Analysis and optimization of Robin-Robin partitioned procedures in fluid-structure interaction problems. *SIAM J. Numer. Anal.*, 48(6):2091–2116, 2010.
- [25] G. Guidoboni, R. Glowinski, N. Cavallini, and S. Canic. Stable loosely-coupled-type algorithm for fluid-structure interaction in blood flow. *J. Comput. Phys.*, 228(18):6916–6937, 2009.
- [26] P. Hansbo, J. Hermansson, and T. Svedberg. Nitsche’s method combined with space-time finite elements for ALE fluid-structure interaction problems. *Comput. Methods Appl. Mech. Engrg.*, 193(39-41):4195–4206, 2004.
- [27] F. Hecht. New development in FreeFem++. *J. Numer. Math.*, 20(3-4):251–265, 2012.
- [28] P. Le Tallec and J. Mouro. Fluid structure interaction with large structural displacements. *Comput. Meth. Appl. Mech. Engrg.*, 190:3039–3067, 2001.
- [29] F. Nobile and C. Vergara. An effective fluid-structure interaction formulation for vascular dynamics by generalized Robin conditions. *SIAM J. Sci. Comput.*, 30(2):731–763, 2008.
- [30] O. Oyekole, C. Trenchea, and M. Bukač. A second-order in time approximation of fluid-structure interaction problem. *SIAM J. Numer. Anal.*, 56(1):590–613, 2018.
- [31] A. Quaini and A. Quarteroni. A semi-implicit approach for fluid-structure interaction based on an algebraic fractional step method. *Math. Models Methods Appl. Sci.*, 17(6):957–983, 2007.
- [32] L. R. Scott and S. Zhang. Finite element interpolation of nonsmooth functions satisfying boundary conditions. *Mathematics of Computation*, 54(190):483–493, 1990.
- [33] A. Seboldt and M. Bukač. A non-iterative domain decomposition method for the interaction between a fluid and a thick structure, 2020.
- [34] S. Čanić, B. Muha, and M. Bukač. Stability of the kinematically coupled β -scheme for fluid-structure interaction problems in hemodynamics. *Int. J. Numer. Anal. Model.*, 12(1):54–80, 2015.

APPENDIX A. PROOF OF LEMMA 4.4

Proof. We begin this proof by establishing several identities. The first identity follows from Minkowski’s integral inequality and Jensen’s inequality. Namely, we note that for any H^ℓ -norm $\|\cdot\|$, we have

$$(A.1) \quad \left\| \frac{1}{\Delta t} \int_{t_n}^{t_{n+1}} w(\cdot, s) ds \right\|^2 \leq \frac{1}{\Delta t} \int_{t_n}^{t_{n+1}} \|w(\cdot, s)\|^2 ds.$$

Our remaining identities are straightforward to prove. Let $|r| \leq 2$ and define

$$\bar{w}^{n+1}(x) := \frac{1}{\Delta t} \int_{t_n}^{t_{n+1}} w(x, s) ds.$$

We have

$$(A.2) \quad \partial_x^r (w^{n+1} - w^n) = \int_{t_n}^{t_{n+1}} \partial_x^r (\partial_t w)(\cdot, s) ds,$$

$$(A.3) \quad \partial_x^r (\partial_{\Delta t} w^{n+1} - \partial_t w^{n+1/2}) = \frac{1}{2\Delta t} \int_{t_n}^{t_{n+1}} (t_{n+1} - s)(s - t_n) \partial_x^r \partial_t^3 w(\cdot, s) ds,$$

$$(A.4) \quad \partial_{\Delta t} w^{n+1} - \partial_t w^{n+1} = \frac{-1}{\Delta t} \int_{t_n}^{t_{n+1}} (s - t_n) \partial_t^2 w(\cdot, s) ds,$$

$$(A.5) \quad \partial_x^r (w^{n+1} - \bar{w}^{n+1}) = \frac{1}{\Delta t} \int_{t_n}^{t_{n+1}} (s - t_n) \partial_x^r (\partial_t w)(\cdot, s) ds,$$

$$(A.6) \quad \partial_x^r (w^{n+1/2} - \bar{w}^{n+1}) = \frac{-1}{2\Delta t} \int_{t_n}^{t_{n+1}} (t_{n+1} - 2s + t_n) \partial_x^r (\partial_t w)(\cdot, s) ds.$$

We may now proceed with the proof of Lemma 4.4.

To prove (4.14a), we write $\partial_{\Delta t} R_h^s \mathbf{q}^{n+1} - \partial_t \mathbf{q}^{n+1/2} = (R_h^s - I) \partial_{\Delta t} \mathbf{q}^{n+1} + (\partial_{\Delta t} \mathbf{q}^{n+1} - \partial_t \mathbf{q}^{n+1/2})$ and

$$\partial_{\Delta t} \mathbf{q}^{n+1} = \frac{1}{\Delta t} \int_{t_n}^{t_{n+1}} (\partial_t \mathbf{q})(\cdot, s) ds.$$

Hence,

$$(R_h^s - I) \partial_{\Delta t} \mathbf{q}^{n+1} = \frac{1}{\Delta t} \int_{t_n}^{t_{n+1}} (R_h^s - I) (\partial_t \mathbf{q})(\cdot, s) ds.$$

It therefore follows from (A.1) and (4.4) that

$$(A.7) \quad \|(R_h^s - I) \partial_{\Delta t} \mathbf{q}^{n+1}\|_{L^2(\Omega_s)}^2 \leq \frac{1}{\Delta t} \int_{t_n}^{t_{n+1}} \|(R_h^s - I) (\partial_t \mathbf{q})(\cdot, s)\|_{L^2(\Omega_s)}^2 ds \leq \frac{Ch^4}{\Delta t} \int_{t_n}^{t_{n+1}} \|\partial_t \mathbf{q}(\cdot, s)\|_{H^2(\Omega_s)}^2 ds.$$

To estimate $\partial_{\Delta t} \mathbf{q}^{n+1} - \partial_t \mathbf{q}^{n+1/2}$, we apply Hölder's inequality to (A.3) with $|r| = 0$ to obtain

$$\begin{aligned} |\partial_{\Delta t} \mathbf{q}^{n+1} - \partial_t \mathbf{q}^{n+1/2}| &\leq \left(\frac{1}{4\Delta t^2} \int_{t_n}^{t_{n+1}} (t_{n+1} - s)^2 (s - t_n)^2 ds \right)^{1/2} \left(\int_{t_n}^{t_{n+1}} |\partial_t^3 \mathbf{q}(\cdot, s)|^2 ds \right)^{1/2} \\ &= \left(\frac{\Delta t^3}{5!} \right)^{1/2} \left(\int_{t_n}^{t_{n+1}} |\partial_t^3 \mathbf{q}(\cdot, s)|^2 ds \right)^{1/2}. \end{aligned}$$

Therefore,

$$(A.8) \quad \|\partial_{\Delta t} \mathbf{q}^{n+1} - \partial_t \mathbf{q}^{n+1/2}\|_{L^2(\Omega_s)}^2 \leq \frac{\Delta t^3}{5!} \int_{t_n}^{t_{n+1}} \|\partial_t^3 \mathbf{q}(\cdot, s)\|_{L^2(\Omega_s)}^2 ds.$$

To get the estimate (4.14b), we recall that $\boldsymbol{\lambda}^{n+1} = \sigma_f(\mathbf{u}^{n+1}, p^{n+1}) \mathbf{n}$. Then, we use a trace inequality (4.3) to get

$$\begin{aligned} \|\boldsymbol{\lambda}^{n+1} - \boldsymbol{\lambda}^n\|_{L^2(\Sigma)}^2 &\leq C \|\sigma_f(\mathbf{u}^{n+1}, p^{n+1}) \mathbf{n} - \sigma_f(\mathbf{u}^n, p^n) \mathbf{n}\|_{H^1(\Omega_f)}^2 \\ &\leq C \left(\mu^2 \|\epsilon(\mathbf{u}^{n+1} - \mathbf{u}^n)\|_{H^1(\Omega_f)}^2 + \|p^{n+1} - p^n\|_{H^1(\Omega_f)}^2 \right). \end{aligned}$$

Applying (A.1) and (A.2), we obtain our result.

The bound for (4.14c) follows in the same manner with an additional application of (4.2).

Similarly, (4.14d) follows immediately from (A.3) and (A.1) after applying the trace inequality (4.3) and the stability result (4.2).

To get the bound (4.14e) we write $\partial_{\Delta t} R_h^f \mathbf{u}^{n+1} - \partial_t \mathbf{u}^{n+1} = (R_h^f - I) \partial_{\Delta t} \mathbf{u}^{n+1} + \partial_{\Delta t} \mathbf{u}^{n+1} - \partial_t \mathbf{u}^{n+1}$. Similar to the bound (A.7), we can show that

$$\|(R_h^f - I) \partial_{\Delta t} \mathbf{u}^{n+1}\|_{L^2(\Omega_f)}^2 \leq \frac{Ch^4}{\Delta t} \left(\int_{t_n}^{t_{n+1}} \|\partial_t \mathbf{u}(\cdot, s)\|_{H^2(\Omega_f)}^2 ds \right).$$

Furthermore, applying (A.5) and Hölder's inequality, we establish

$$\|\partial_{\Delta t} \mathbf{u}^{n+1} - \partial_t \mathbf{u}^{n+1}\|_{L^2(\Omega_f)}^2 \leq \frac{\Delta t}{3} \int_{t_n}^{t_{n+1}} \|\partial_t^2 \mathbf{u}(\cdot, s)\|_{L^2(\Omega_f)}^2 ds.$$

Combining the above two inequalities gives (4.14e).

For (4.14f), we use (4.2) and write

$$\|\nabla R_h^s \mathbf{g}_2^{n+1}\|_{L^2(\Omega_s)}^2 \leq C \|\mathbf{g}_2^{n+1}\|_{H^1(\Omega_s)}^2.$$

The bound now follows exactly that of (4.14d).

In order to prove (4.14g) we bound each term in \mathbf{g}_1^{n+1} separately. To bound the term $\alpha(\partial_{\Delta t} R_h^s \boldsymbol{\eta}^{n+1} - R_h^f \mathbf{u}^{n+1})$ we use that $\mathbf{u}^{n+1} = \partial_t \boldsymbol{\eta}^{n+1}$ on Σ , indicating that $R_h^f \mathbf{u}^{n+1} = R_h^s \partial_t \boldsymbol{\eta}^{n+1}$. Therefore

$$\alpha(\partial_{\Delta t} R_h^s \boldsymbol{\eta}^{n+1} - R_h^f \mathbf{u}^{n+1}) = \alpha(\partial_{\Delta t} R_h^s \boldsymbol{\eta}^{n+1} - \partial_t R_h^s \boldsymbol{\eta}^{n+1}).$$

Thus, applying the trace inequality (4.3) and stability (4.2), we have

$$\alpha^2 \|\partial_{\Delta t} R_h^s \boldsymbol{\eta}^{n+1} - \partial_t R_h^s \boldsymbol{\eta}^{n+1}\|_{L^2(\Sigma)}^2 \leq C \alpha^2 \|\partial_{\Delta t} \boldsymbol{\eta}^{n+1} - \partial_t \boldsymbol{\eta}^{n+1}\|_{L^2(t_n, t_{n+1}; H^1(\Omega_s))}^2.$$

Therefore, applying (A.4) and using Hölder's inequality, we have

$$\alpha^2 \|\partial_{\Delta t} R_h^s \boldsymbol{\eta}^{n+1} - \partial_t R_h^s \boldsymbol{\eta}^{n+1}\|_{L^2(\Sigma)}^2 \leq C \alpha^2 \Delta t \int_{t_n}^{t_{n+1}} \|\partial_t^2 \boldsymbol{\eta}(\cdot, s)\|_{H^1(\Omega_s)}^2 ds.$$

Combining this with (4.14d) gives (4.14g).

Next, the proofs for (4.14h) and (4.14i) are nearly identical, so we only provide the proof of (4.14h). Recall from (4.4) that

$$\|S_h p^{n+1} - p^{n+1}\|_{L^2(\Omega_f)}^2 \leq Ch^4 \|p^{n+1}\|_{H^2(\Omega_f)}^2.$$

We may then write $p^{n+1} = p^{n+1} - \bar{p}^{n+1} + \bar{p}^{n+1}$. Thus we have

$$\|S_h p^{n+1} - p^{n+1}\|_{L^2(\Omega_f)}^2 \leq Ch^4 \left(\|p^{n+1} - \bar{p}^{n+1}\|_{H^2(\Omega_f)}^2 + \|\bar{p}^{n+1}\|_{H^2(\Omega_f)}^2 \right).$$

Then, using (A.5) (A.1), along with Hölder's inequality, we have

$$\begin{aligned} \|p^{n+1} - \bar{p}^{n+1}\|_{H^2(\Omega_f)}^2 &\leq C \Delta t \|\partial_t p\|_{L^2(t_n, t_{n+1}; H^2(\Omega_f))}^2, \\ \|\bar{p}^{n+1}\|_{H^2(\Omega_f)}^2 &\leq C \frac{1}{\Delta t} \|p\|_{L^2(t_n, t_{n+1}; H^2(\Omega_f))}^2. \end{aligned}$$

Our result then follows from combining the terms above.

For (4.14j), we use the stability result (4.2) to recognize that $\|\nabla S_h p^{n+1}\|_{L^2(\Omega_f)} \leq C \|p^{n+1}\|_{H^1(\Omega_f)}$. We may then follow the proof of (4.14h) to write

$$\|\nabla S_h p^{n+1}\|_{L^2(\Omega_f)}^2 \leq C \left(\|p^{n+1} - \bar{p}^{n+1}\|_{H^1(\Omega_f)}^2 + \|\bar{p}^{n+1}\|_{H^1(\Omega_f)}^2 \right).$$

Following the same process as (4.14h), this yields

$$\|\nabla S_h p^{n+1}\|_{L^2(\Omega_f)}^2 \leq C \left(\Delta t \|\partial_t p\|_{L^2(t_n, t_{n+1}; H^1(\Omega_f))}^2 + \frac{1}{\Delta t} \|p\|_{L^2(t_n, t_{n+1}; H^1(\Omega_f))}^2 \right).$$

In a similar fashion, we bound (4.14k) by writing $\mathbf{u}^{n+1} = \mathbf{u}^{n+1} - \bar{\mathbf{u}}^{n+1} + \bar{\mathbf{u}}^{n+1}$. The result follows in the same manner as (4.14j).

To prove (4.14l), we follow the proof of (4.14h), however we apply (4.5) and (A.6) in place of (4.4) and (A.5). Thus we have

$$\|\nabla(R_h^s - I) \boldsymbol{\eta}^{n+1/2}\|_{L^2(\Omega_s)}^2 \leq Ch^2 \|\boldsymbol{\eta}^{n+1/2}\|_{H^2(\Omega_s)}^2.$$

Thus, noting $\boldsymbol{\eta}^{n+1/2} = \boldsymbol{\eta}^{n+1/2} - \bar{\boldsymbol{\eta}}^{n+1} + \bar{\boldsymbol{\eta}}^{n+1}$, we have

$$\begin{aligned} \|\boldsymbol{\eta}^{n+1/2} - \bar{\boldsymbol{\eta}}^{n+1}\|_{H^2(\Omega_s)}^2 &\leq C \Delta t \|\partial_t \boldsymbol{\eta}\|_{L^2(t_n, t_{n+1}; H^2(\Omega_s))}^2, \\ \|\bar{\boldsymbol{\eta}}^{n+1}\|_{H^2(\Omega_s)}^2 &\leq \frac{1}{\Delta t} \|\boldsymbol{\eta}\|_{L^2(t_n, t_{n+1}; H^2(\Omega_s))}^2. \end{aligned}$$

We then combine terms.

Finally, for (4.14m) we use (A.1) and (4.5), to get

$$\|\nabla(R_h^s - I) \partial_{\Delta t} \boldsymbol{\eta}^{n+1/2}\|_{L^2(\Omega_s)}^2 \leq C \frac{h^2}{\Delta t} \|\partial_t \boldsymbol{\eta}\|_{L^2(t_n, t_{n+1}; H^2(\Omega_s))}^2.$$

□

DEPARTMENT OF MATHEMATICS, UNIVERSITY COLLEGE LONDON, LONDON, UK-WC1E 6BT, UNITED KINGDOM
Email address: e.burman@ucl.ac.uk

DIVISION OF APPLIED MATHEMATICS, BROWN UNIVERSITY, 182 GEORGE STREET, PROVIDENCE, RI 02912, USA
Email address: rebecca.durst@brown.edu

INRIA PARIS, 75012 PARIS, FRANCE – SORBONNE UNIVERSITE & CNRS, UMR 7598 LJLL, 75005 PARIS, FRANCE
Email address: miguel.fernandez@inria.fr

DIVISION OF APPLIED MATHEMATICS, BROWN UNIVERSITY, 182 GEORGE STREET, PROVIDENCE, RI 02912, USA
Email address: johnny_guzman@brown.edu